Manipulation and Modification of Nanoparticles through Mechanical Deformation

by

Brandon Harrison Smith

B. A. in Chemistry, Washington and Jefferson College, 2011

Submitted to the Graduate Faculty of the

Kenneth P. Dietrich School of Arts and Sciences in partial fulfillment

of the requirements for the degree of

Master of Science

University of Pittsburgh

2013

UNIVERSITY OF PITTSBURGH

Dietrich School of Arts and Sciences

This thesis was presented

by

Brandon Harrison Smith

It was defended on

November 25, 2013

and approved by

Dr. Tara Meyer, Associate Professor, Department of Chemistry

Dr. Alexander Star, Associate Professor, Department of Chemistry

Thesis Advisor: Dr. Jill Millstone, Assistant Professor, Department of Chemistry

Manipulation and Modification of Nanoparticles through Mechanical Deformation

Brandon H. Smith, M.S.

University of Pittsburgh, 2013

Copyright © by Brandon Harrison Smith

2013

Manipulation and Modification of Nanoparticles through Mechanical Deformation

Brandon Harrison Smith, M.S.

University of Pittsburgh, 2013

Nanoparticles are a unique class of materials that exhibit size and shape dependent properties. The goal in this current work is to take advantage of this attribute of nanoparticles through mechanical deformation. Our approach is to use a stimuli responsive template to bend anisotropic gold nanoparticle. This approach will entail the use of a silica nanoparticle core from which polyNIPAM, a polymer that exhibits a lower critical solution temperature, will be grown. Then through the use of an avidin-biotin interaction a gold nanoparticle will be attached to the surface. When heated above 32°C the polyNIPAM shell will shrink causing a mechanical defect in the anisotropic nanoparticle as it bends. This approach to deformation will be a high throughput technique that will allow for many anisotropic nanoparticles to be bent at the same time. The induced mechanical defect has potential to change the physical and chemical properties of the nanoparticle. The induced defect site by definition should have a higher chemical reactivity due to the straining of bonds at that point on the particle. If this holds true then we can take advantage of this higher chemical reactivity and make new bifunctional nanoparticles.

TABLE OF CONTENTS

LIST OF TABLES

LIST OF FIGURES

1.0 INTRODUCTION

Nanoparticles exhibit many changes in their properties based on size, shape, composition, and surface functionality.[1,2,3] Numerous examples of each of these already exist. Silver nanoprisms of various sizes have been synthesized and their shift in the resulting localized surface plasmon resonance (LSPR) has been recorded.[4] Gold nanorods and nanoprisms have been synthesized and completely different spectral signatures have been seen in UV-vis-NIR.[5,6,7] Nanoparticle alloys of gold and copper have been synthesized and a shift in their photoluminescence can be seen with increased copper incorporation.[8] Additionally, by performing ligand exchanges with nanoparticles shifts in the UV-Vis-NIR can also be seen.[9,10,11] The more control that can be exhibited over each of these characteristics, the more readily nanoparticles can be adapted to different applications.

Rational shape control, especially anisotropic shape control, requires a detailed understanding of the mechanism by which these particles are made. Many different morphologies have already been synthesized with rods, spheres, wires, and plates being the most well studied and common.[5,6,12,13] However, beyond these basic shapes, little has been accomplished to make more complicated morphologies without using costly and/or intricate methods such as AFM,[14,15] nanomanipulators,[16] lithography,[17] or an "SEMentor".[18] Furthermore, the synthesis of nanoparticles is limited by the material's crystal structure with current methods. Obtaining new morphologies in a high yield and cost efficient manner is necessary for nanoparticles to move from the research stage to broader application. Here it is proposed to use

mechanical deformation as a way to rationally control nanocrystal shape and access new architectures.

1.1 MECHANICAL DEFORMATION

1.1.1 Definition of mechanical deformation

Mechanical deformation is the act of applying a force to a material to the point that the material buckles in some form. The force that the material feels is known as stress[19] and for the purposes of these experiments can be defined in terms of tensile strength since a bend is essentially an elongation. For a tensile strength, stress is applied by applying force on either end of an object. This is different from shear and torsional strength where the stress is applied in the form of opposite torques or twists at its ends. Stress can therefore be defined by the equation:

$$\sigma = \frac{F}{A_0}$$

where σ is engineering stress which is the normalized load to minimize geometrical factors, F is the instantaneous force or load applied to the specimen cross-section, and A_0 is the original cross-sectional area of the material.[19] When stress is applied the material will feel a strain on its structure. This strain exhibited by the material can be defined by the equation:

$$\epsilon = \frac{l_i - l_0}{l_0}$$

where ε is engineering strain which is the normalized elongation to minimize geometrical factors, l_i in the instantaneous length of the material, and l_0 is the original length.[19] The strain exhibited by a material and the amount that it deforms is directly proportional to the magnitude

of stress produced, at least for most metals at relatively low levels of stress.[19] This gives Hooke's law:

$$\sigma = E\epsilon$$

where E is the modulus of elasticity or Young's modulus. Young's modulus is simply a constant of proportionality between stress and strain. This value is completely dependent on the material under stress and therefore is different for any given material.[19] Deformation that follows this proportionality of stress and strain is known as elastic deformation. Elastic deformation is nonpermanent, and once the stress is removed, the material will return to its initial shape. On an atomic scale, this corresponds to small changes in interatomic spacing and stretching of atomic bonds.[19] The changes in spacing and stretching of the chemical bonds would revert back to their original state when the stress is removed. When stress is no longer proportional to strain it is known as plastic deformation. On an atomic scale, this corresponds to the actual breaking of bonds and the forming of new bonds.[19] Thus, once the stress is removed, the material cannot return to its original shape. These new bonds will be more strained than the shape of the original material and will result in a more chemically reactive surface at the point of deformation, known as the defect site.

1.1.2 Application to nanoparticles for more chemically reactive sites

Defect sites induced by mechanical deformation should be more chemically reactive than their terrace site counterparts.[20] At the defect sites, bonds should be strained, and strained surface bonds should have higher surface energy. Higher surface energy equates to a more chemically reactive surface. This increased chemical reactivity can be strategically used, and reactions can

take place selectively at the defect site. Therefore, inducing defect sites will allow access to previously inaccessible part, of nanostructures to make novel architectures.

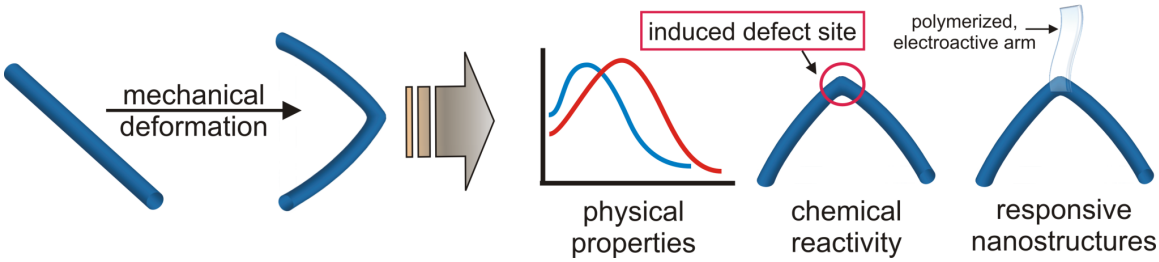

Figure 1. The potential effects of inducing mechanical deformation. By inducing mechanical deformation, not only are changes in its physical shape evident but also new modes of chemical reactivity on the nanoparticle. This reactivity can then be used to access a previously inaccessible part of the nanostructures.

1.1.3 Alternative modes of applying mechanical stress to nanoparticle

Several attempts have previously been made to mechanically apply stress to a nanoparticle. Using an AFM tip, particles can physically be bent one at a time. The Wang et al. were able to measure the modulus elasticity of individual ZnO nanowires and nanotubes.[14] The technique requires simultaneously recording the topography and lateral force image in AFM contact mode when the AFM tip scans across the aligned nanowires. Various other techniques using AFM to manipulate nanowires and nanotubes also exist. Lieber et al. were able to affix carbon nanotubes onto a substrate and then at the other end, deflect it with the AFM tip and calculate the elastic modulus from the force-deflection curve.[21] Yu et al. attached two AFM tips onto either side of a carbon nanotube and then pulled the nanotube, causing it to stretch, and its tensile strength and modulus of elasticity could be determined.[22] Lastly, Salvetat et al. developed a technique of physically bending carbon nanotubes using an AFM tip.[23,24] These AFM tip methods, although effective, are not reasonable to perform on a bulk scale since each particle must be bent individually. Similarly, work has also been done using an SEMentor by Jang and Greer.[18] Here, samples are studied inside an SEM equipped with tensile grips allowing for *in situ*

mechanical deformation. These studies allowed for the determination of engineering stress and strain. Again, this method of performing mechanical deformation must be done particle by particle, so high throughput is not possible. High throughput solution phase methods have also been studied. Wang et al. has been able to produce bends in gold nanowires by stirring during synthesis.[25] The resulting kinked gold wires could then be studied for their pronounced near-IR absorption and SERS properties.[26] Overall, these methods have added much to the study of mechanical deformation of nanoparticles, and this work hopes to contribute more to the field through a new approach.

1.2 TEMPLATED APPROACH TO MECHANICAL DEFORMATION

1.2.1 System to be investigated

The approach attempted here will be to use a stimuli responsive bead template to bend anisotropic nanoparticles. As shown in **Figure 2**, the bead template and the nanoparticle will have an attraction to each other such that the nanoparticle will attach conformally. Following attachment the bead will respond to a stimuli causing it to shrink and assuming that the attraction between the bead and the nanoparticle is strong enough to remain attached bending will occur.

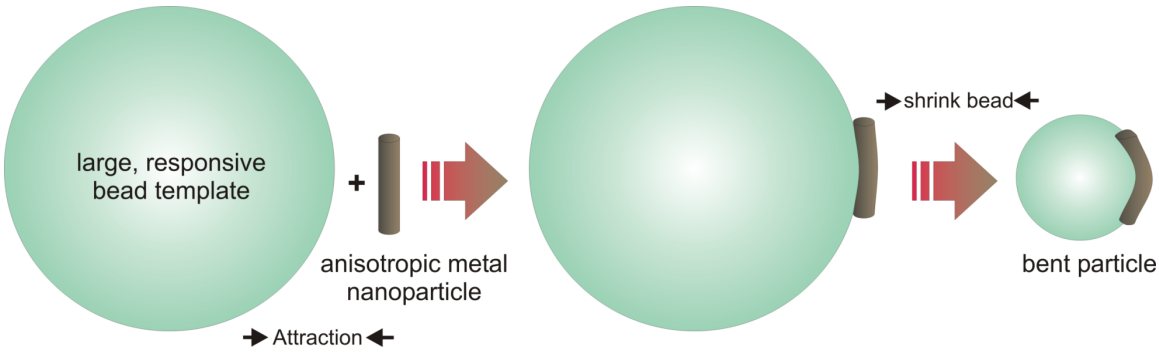

Figure 2. Stimuli responsive bead template attaching to an anisotropic metal nanoparticle such as a rod and then shrinking in an effort to bend said rod.

The bead template will consist of monodisperse particles with well-understood surface chemistry. In addition, these particles will be robust, and therefore the particle integrity will not be affected by reactions performed around it. From the bead template, a stimuli responsive shell will be grown. This shell will have a significant change in volume when exposed to an applied external stimulus. This will result in a high throughput method with tunable deformation.

1.2.2 Silica bead core

Silica beads were chosen as the core for the system to the templated approach. Silica nanoparticles are a well-understood class of nanoparticles that have been studied for several decades.[27,28,29] Using the Stöber method, monodisperse populations of various sizes can be made with relative ease.[30] This sol-gel process works by first hydrating the monomer units and then using a condensation reaction to combine individual silica units.

$$Si(OR)_4 + H_2O \rightarrow SiO_2 + 4ROH$$

Figure 3. Overall reaction in the sol-gel process.

Using this method also gives a surface chemistry that is easily tunable. By adding new monomer units that contain other functional groups to existing particles, particles with different surface chemistry can be synthesized.[28]

1.2.3 PolyNIPAM

Poly(*N*-isopropylacrylamide) (polyNIPAM) is a temperature-responsive polymer that exhibits an lower critical solution temperature (LCST). An LCST is a temperature at which a material, particularly polymers, exhibits a transition from being miscible in solution to being immiscible.[31] When heated in water above 32°C, polyNIPAM undergoes a reversible LCST phase transition from a swollen hydrated state to a shrunken dehydrated state, losing about 90% of its volume in the process.[32,33] In addition, this transition can be reversed multiple times making polyNIPAM a very robust material for this class of polymers.[34] This heat-induced phase transition exhibited by aqueous polyNIPAM solutions is not unique, as many other water-soluble polymers exhibit LCSTs. However, others lack the sharpness of the transition, a transition temperature that is biologically relevant since it is close to body temperature, the robustness of the polymer itself, and the availability of information on the polymer and its phase transition.[35] For these reasons, polyNIPAM was chosen as the stimuli responsive shell for the system being created.

1.2.3.1 Atom transfer radical polymerization

PolyNIPAM can be synthesized by a variety of polymerizations,[36,37] but for this work, atom transfer radical polymerization (ATRP) was chosen. ATRP has several benefits that make it useful for the needs of this work. ATRP is known as a living polymerization, meaning the ability

of the polymer chain to terminate has been removed.[38] ATRP is not a perfect living polymerization, but it does allow for high molecular weight polymers with low polydispersity.[39] High molecular weight chains will result in a thick shell around the silica bead template. The thicker the shell the more the volume will decrease when exposed to the stimulus. The uniform polymer chain growth, which leads to low polydispersity, stems from the transition metal-based catalyst. ATRP reactions are very robust in that they are tolerant of many functional groups like allyl, amino, epoxy, hydroxyl, and vinyl groups present in either the monomer or the initiator.[40] ATRP methods are also advantageous due to the ease of preparation, commercial availability, and inexpensive catalysts and initiators.[41]

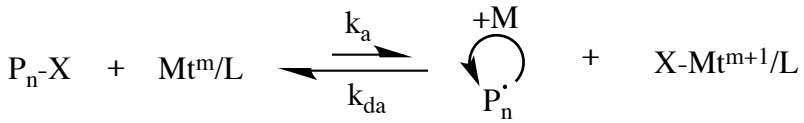

Figure 4. Mechanism of ATRP where P_n is the polymer chain, X is a halide initiator, Mt is a transition metal, L is the ligands surrounding the metal, and M is an additional monomer unit.

This catalyst provides an equilibrium between an active propagating species and an inactive dormant state, as shown in the above mechanism. Since the dormant state of the polymer is highly preferred in this equilibrium, only a few monomer units are added at a time. This slow rate of propagation is responsible for the low polydispersity due to the fact that the chains polymerized are of a uniform length.[41] This equilibrium, in turn, lowers the concentration of propagating radicals, therefore suppressing unintentional termination and controlling molecular weights.

There are five important factors to consider with ATRP: the monomer unit, the initiator, the catalyst, the solvent, and temperature. Monomers suitable for ATRP need to be able to stabilize the free radical formed.[42] Examples include styrenes, acrylates, and acrylamides. The number of growing polymer chains is determined by the initiator. The faster the initiation, the

fewer terminations and chain transfers, the more consistent the number of propagating chains leading to narrow molecular weight distributions.[43] Most initiators for ATRP are alkyl halides.[44] Alkyl halides, such as alkyl bromides, are more reactive than alkyl chlorides, although both have good molecular weight control.[43] Organic halides that are similar in the organic framework as the propagating radical are often chosen as initiators. The shape or structure of the initiator can determine the architecture of the polymer.[45] The catalyst is the most important component of ATRP because it determines the equilibrium constant between the active and dormant species. This equilibrium determines the polymerization rate, and an equilibrium constant too small may inhibit or slow the polymerization, while an equilibrium constant too large leads to a high distribution of chain lengths.[44] There are therefore several requirements of the metal catalyst there needs to be two accessible oxidation states that are separated by one electron, the metal center needs to have a reasonable affinity for halogens, the coordination sphere of the metal needs to be expandable when it's oxidized so to accommodate the halogen, and the metal needs to have a strong ligand complexation.[43] Solvent and temperature are the least important, but can be used to further tune the reaction based on the particular polymer.

1.2.4 Gold nanoprisms

The final piece to the system being built is an anisotropic gold nanoprism. A gold nanoprism would be superior to a gold nanorod due to its higher aspect ratio. In addition, gold nanoparticles are a well studied class of materials.[5,6,7] Thus, gold particles are stable and should not deteriorate during these experiments. Gold anisotropic nanoparticles, such as nanoprisms, are ideal materials to study because they exhibit optoelectronic properties that can serve as diverse and sensitive readouts,[46,47,48] and possess tailorable surface chemistries.[49,50] An anisotropic

nanoparticle is necessary because a much smaller force is necessary to bend an anisotropic nanoparticle compared to an isotropic one. This is due to the fact that the force necessary is inversely proportional to the length of the nanoparticle. As shown with the equation:

$$F = \frac{\pi^2 EI}{L^2}$$

where, F is the force necessary to bend an object, E is the Young's modulus for the material, I is the moment of inertia for a given cross-sectional area and L is the length of the object. Therefore an anisotropic particle with the same cross-sectional area would take less force to bend. In addition, the longer the particle in comparison to its cross-sectional area the less force necessary to bend it.

1.2.4.1 Determining thermal fluctuations of gold nanoprisms

In order to determine the optimal size of the stimuli responsive bead template, studies must first be conducted to determine the thermal fluctuation of the anisotropic gold nanoparticles. The nanoparticles in solution should have some thermal fluctuation that will allow them to attach to a curved surface. The initial studies help to determine the bead size and the attraction type that will be used in the desired system. In these studies, the bead size will be varied to determine the minimum diameter for gold nanoprism attachment. This size will depend on the inherent thermal fluctuations of the gold nanoparticle as well as the strength of the attraction between the gold nanoparticle and the template surface. Three distinct possibilities can be envisioned for when anisotropic gold nanoparticles are added to beads in solution.

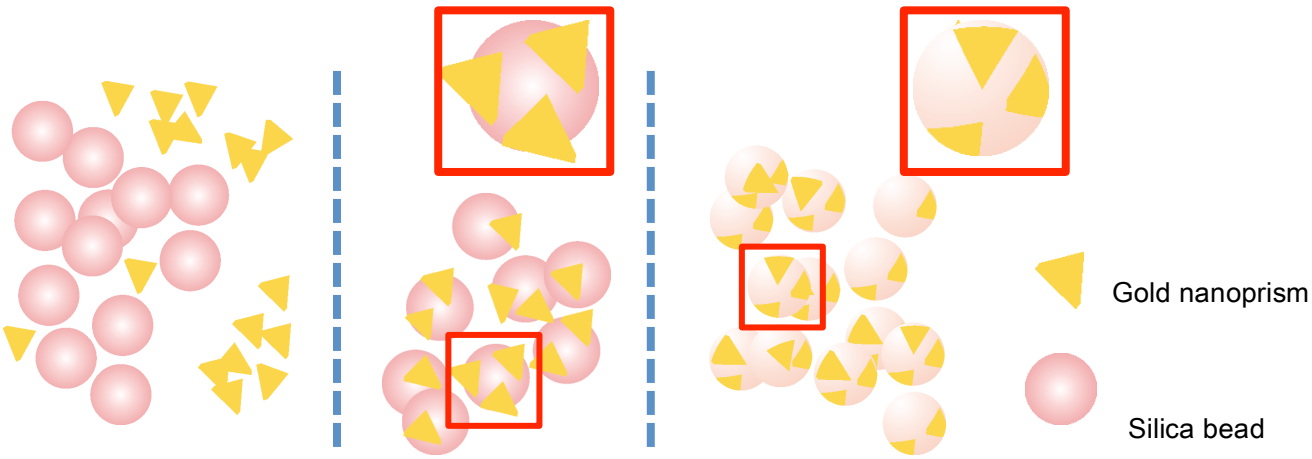

Figure 5. Possible outcomes for addition of gold nanoprisms with silica beads; no attachment (left), nonconformal attachment (middle), conformal attachment (right).

As shown in **Figure 5** the three possibilities are no attachment where the silica beads and the gold nanoprisms stay separate, nonconformal attachment where the beads and nanoprisms attach, but do not wrap around the surface of the bead, and conformal attachment where the beads attach and wrap around the bead surface. To be able to bend the gold nanoprisms conformal attachment is required since this is the scenario of complete attachment to the bead surface. Therefore, it is necessary to determine a bead size range at which this type attachment happens.

1.3 OBJECTIVES

As discussed previously, mechanical deformation should allow for the rational design of new nanoparticle shapes as well as nanoparticles with multiple functionalities within the same particle. While there exist many ways to synthesize nanoparticles, few do so in a rational manner. This project will attempt to build a system consisting of a robust silica core, a stimuli responsive shell consisting of polyNIPAM, and a gold nanoparticle with the intention of bending the gold nanoparticle. The first step in this study will be a set of preliminary experiments to

determine the thermal fluctuations of the gold nanoprism in solution. In other words, the minimum diameter of a bead that a nanoprism will attach given a certain interaction type between it and the bead surface needs to be determined. Synthesizing several silica beads of varying sizes and interaction types as well as verification of conformal attachment via scanning electron microscopy (SEM) will determine this. The second step of the study will be to synthesize and characterize the stimuli responsive particles. The stimuli responsive bead will be characterized by techniques typically used by both a nanochemist and a polymer chemist, meaning that attributes like particle size, morphology, and surface functionality will be determined by transmission electron microscopy (TEM), dynamic light scattering (DLS), Zeta Potential, fourier transform infrared spectroscopy (FTIR), and nuclear magnetic resonance (NMR); and characteristics like molecular weight, polydispersity, chain length, and terminal group will be determined by gel permutation chromatography (GPC) and matrix assisted laser desorption ionization (MALDI). The final step will be to change the terminal group at the end of the polymer for attachment of the gold nanoprisms to make the bending of the nanoprisms possible.

2.0 EXPERIMENTAL

2.1 MATERIALS

(3-Aminopropyl)trimethoxysilane (APTMS, 97%), (3-mercaptopropyl)trimethoxysilane (MPTMS, 95%), α-bromoisobutyryl bromide (98%), 2-propanol (IPA, 99.90%), 4-(dimethylamino)pyridine (DMAP, 99%), ammonium hydroxide (28-30%), biotin (>99%), copper (I) chloride (99.995%), copper (II) chloride (99.99%), cetyltrimethylammonium bromide (CTAB, 99%), dichloromethane (CH_2Cl_2, >99.8%), hydrofluoric acid (HF, 48%), Hydrogen tetrachloroaurate(III) trihydrate ($HAuCl_4 \cdot 3H_2O$, 99.999%), L-ascorbic acid (ascorbic acid, >99%), N-isopropylacrylamide (NIPAM, 99%), N,N'-Dicyclohexylcarbodiimide (DCC, 99%), N,N-Dimethylformamide (DMF, 99.8%), Ninhydrin (%), Poly(sodium 4-styrenesulfonate) (PSS, 30 wt %), Polyvinylpyrrolidone (PVP, MW=40,000), propargylamine (98%), pyridine (99.8%), silver nitrate ($AgNO_3$, 99.9999%), sodium azide (NaN_3, 99.9%), sodium borohydride ($NaBH_4$, 99.99%), sodium citrate tribasic dihydrate (citrate, ≥99%), Sodium hydroxide (NaOH, 99.99%), sodium iodide (NaI, 99.999%), tetraethoxysilane (TEOS, 99.999%), toluene (99.8%), and Tris[2-(dimethylamino)ethyl]amine (Me_6TREN, 97%) were purchased from Sigma-Aldrich (St. Louis, MO). Ethanol (200 proof) was purchased from Decon Labs, Inc. (King of Prussia, PA). Dueterated-dimethyl sulfoxide (DMSO, >99%) was purchased from Cambridge Isotope Laboratories, Inc. (Tewksbury, MA). All reagents were used as received unless otherwise

indicated. NANOpure (Thermo Scientific, > 18.2 MΩ · cm) water was used in the preparation of all solutions. Before use, all glassware and Teflon coated stir bars were washed with aqua regia (3:1 ratio of concentrated HCl and HNO_3 by volume) and rinsed thoroughly with NANOpure water. *Caution: Aqua regia is highly toxic and corrosive and requires proper personal protective equipment. Aqua regia should be handled in a fume hood only.*

2.2 CHARACTERIZATION METHODS

2.2.1 Sample preparations and methods for DLS and Zeta Potential measurements

Samples were run on a Malvern Zetasizer Nano ZS90 equipped with zeta potential cell. All samples were prepared by making a dilute solution containing particles and then performing further dilutions until repeat measurements were obtained. Data was then worked up using OriginPro 8.5 software to produce resulting graphs.

2.2.2 Sample preparations and methods for TEM

Samples were examined on a FEI Morgagni 268 operating at 80 kV. Samples were prepared by taking 50 μL of as synthesized solution of particles and dispersing in 10 mL of water. From the resulting solution 10 μL were dropped onto a formvar-coated copper transmission electron microscopy (TEM) grid (Ted Pella, Inc.). Samples were allowed to slowly air, dry then were dried under vacuum before characterization.

2.2.3 Sample preparation and methods for UV-Vis-NIR spectroscopy

Samples were prepared for the ninhydrin test by dispersing particles in water and then adding the ninhydrin reagent. The solutions were then heated on a hot plate set to 50°C to accelerate the reaction. The resulting solutions were diluted so as to obtain a transparent solution appropriate for running on UV-Vis-NIR spectrometer. The samples were run on Cary 5000 Spectrophotometer.

2.2.4 Sample preparation and methods for FTIR

Samples were prepared by dispersing particles in an appropriate solvent, usually ethanol. This solution was then dropped onto salt plates, which were run on Bruker Vertex 7-Spectrometer.

2.2.5 Sample preparation and methods for GPC and MALDI measurements

Samples were prepared by etching the silica with HF (*vide infra*) and then dried on a hot plate. For GPC, 5 mg were dissolved in 5 mL of THF, and the resulting solution was run through a Whatman polypropylene 0.45 micron filter. The solution was then run on a Waters 515 HPLC pump and 2414 refractive index detector to determine moleculer weight and polydispersity. For MALDI, samples were dissolved in THF to make a 0.2 mg/mL solution. The matrix solution consisted of 50% (v/v) acetonitrile in water, 5mg/mL α-cyano-4-hydroxycinnamic acid, and 0.1% (v/v) phosphoric acid. 0.5 μL of the matrix solution was mixed with 0.5 μL sample solution

directly on the stainless steel target plate. This sample was then run on a Voyager DE-STR MALDI-TOF.

2.2.6 Purification of polyNIPAM coated silica beads using dialysis tubes

A 2.0 g. sample of polyNIPAM coated silica beads was dispersed in 10 mL of water and then the resulting solution was put into a Float-a-lyzer G2 (MWCO is 3.5-5 kD) dialysis tube. The dialysis tubes were put into a beaker filled with NANOpure water and left under a slow stirring at 100 rpm for 3 weeks making sure to change the water every few days before further functionalization.

2.3 SYNTHESIS OF SEED-MEDIATED GOLD NANOPRISM

Seed-mediated gold nanoprisms were made using a previously developed procedure.[6] First, a seed solution was synthesized. 36 mL of water was added to a 100 mL RBF and set to stir vigorously. To this solution, 1 mL of 0.01 M sodium citrate tribasic dihydrate, 1 mL of 0.01 M $HAuCl_4$, and 1 mL of 0.1 M $NaBH_4$ were added quickly. The solution was then allowed to stir for 1 minute. This seed solution was allowed to age for 2-6 hours. For the next step, 200 mL of a 0.05 M CTAB solution containing 0.05 mM NaI was prepared. Next, several growth solutions were prepared, the first in a 500 mL RBF and the other two in vials. First, 90 mL of the CTAB solution was added to the RBF and 9 mL to each of the vials. Next, to the RBF, 2.5 mL of 0.01 M $HAuCl_4$, 0.5 mL of 0.1 M NaOH, and 0.5 mL of 0.1 M ascorbic acid were added, and similarly, 250 μL of 0.01 M $HAuCl_4$, 50 μL of 0.1 M NaOH, and 50 μL of 0.1 M ascorbic acid

were added to each of the vials. Finally, 1 mL of seed solution was added to the first vial. This was swirled and 1 mL of this solution was quickly added to the second vial. Again, this was swirled and the entire vial was quickly added to the RBF. This was swirled and then allowed to sit for 30 minutes. The resulting purple solution was separated into Eppindorf tubes and allowed to sit overnight. The following day, the supernatant was removed, and a pellet containing prisms was obtained. This was washed twice with water to remove excess CTAB by centrifugation (Eppendorf 5424 centrifuge) at 2,000 rpm for 5 minutes and suspended in water.

2.3.1 Ligand exchange of CTAB-functionalized gold nanoprisms with PVP and PSS

20 mL of nanoprisms, prepared by the procedure outlined above, were transferred into 1 mL Eppindorf tubes and centrifuged at 7,500 rpm for 5 minutes. The resulting pellets were concentrated by dispersing in 5 mL of a 5% w/v PVP in ethanol solution. This solution was allowed to stir at 500 rpm overnight at room temperature. The next day, the nanoprisms were centrifuged at 9,000 rpm for 5 minutes. The pellet obtained was washed three times with ethanol and then dispersed in 1 mL of ethanol. An identical procedure was done using PSS.

2.4 SYNTHESIS OF SILICA BEADS

Silica beads were prepared using a modified Stöber method synthesis.[30] In a typical reaction, two Falcon tubes (A and B) were obtained. To A, 6 mL of water and 17.4 mL of ethanol were added, while 6 mL of TEOS and 10 mL of ethanol was added to tube B. Then in a vial, 10 mL of ethanol were combined with 0.6 mL of ammonium hydroxide. Falcon tubes A and

B were combined in a 500 mL round bottom flask (RBF) equipped with a magnetic stir bar and set to stir for several seconds to mix. Then the vial containing the ammonium hydroxide solution was added, and the solution was allowed to stir overnight (approximately 14 hours). For different size, particles the amount of ammonium hydroxide could be changed, with increasing ammonium hydroxide concentration corresponding to bigger particles. However, as the volume of ammonium hydroxide was increased, the ethanol volume of falcon tube A was decreased to maintain an overall volume of 50 mL. The following morning the particles were spun down on the centrifuge at 5,000 rpm for 20 minutes. The supernatant was discarded, and the particles were washed three times with ethanol via dissolving the white pellet and centrifugation (Eppendorf 5804R centrifuge) at 5,000 rpm for 20 minutes. The obtained pellet was either dissolved in 45 mL of ethanol for further functionalization or dissolved in a minimal amount of ethanol and transferred to a petri dish on a hot plate set to 50°C to dry overnight for characterization.

2.4.1 Approach

This modified version of the Stöber method was chosen because it led to monodisperse populations of silica particles. By adding the ammonium hydroxide solution immediately after the Falcon tubes were combined allows for one nucleation event. Water on its own is known to be able to nucleate silica particles, but at a much slower rate. Thus, if given time, nucleation can start before the ammonium hydroxide solution is added, and a much larger distribution of particles is created. In addition, the described method allows for control over size. By adding increasing amounts of ammonium hydroxide, a broad range of sizes can be accessed, which is crucial for the initial studies.

2.4.2 Alternative approaches and approach drawbacks

Alternatively, the solution made by combining Falcon tubes A and B was allowed to mix for a few minutes before adding the ammonium hydroxide solution. This originally allowed for sufficient mixing of the solutions to occur. However, this led to a bimodal population of silica spheres due to nucleation starting before the ammonium hydroxide was added. The above approach fixes this problem. However, at higher concentrations of ammonium hydroxide a larger distribution in the population of the obtained silica nanoparticles is observed.

2.5 SURFACE FUNCTIONALIZATION OF SILICA BEADS WITH AMINE GROUPS

Surface functionalization of silica beads with amine groups was completed using a previously reported method.[51,52] A 45 mL solution containing the above prepared silica beads was set to stir at 300 rpm in a RBF equipped with a magnetic stir bar and refluxed at 60°C. Once reflux had begun, 50 μL of ammonium hydroxide was added, followed by 2 mL of APTMS. The reaction was then allowed to reflux overnight (approximately 14 hours). The following morning, the particles were spun down on the centrifuge (Eppendorf 5804R centrifuge) at 5,000 rpm for 20 minutes. The supernatant was discarded, and the particles were washed three times with ethanol via dissolving the white pellet and centrifugation at 5,000 rpm for 20 minutes. At this point, the obtained pellet was either dried similarly to the bare silica beads for characterization or worked up for further functionalization. If for further functionalization, the solution of beads was

washed three times with toluene similarly to previous washings. The final pellet was dissolved in 45 mL of toluene.

2.5.1 Approach

This modified procedure was chosen for its simplicity in obtaining silica nanoparticles functionalized with amine groups at the surface. The APTMS adds directly to the surface of the silica through the same sol-gel method as normal TEOS growth. However, rather than terminating in a hydroxide group which could be used for further growth, the surface terminates in an amine. As with the silica bead synthesis, ammonium hydroxide acts as a catalyst for this reaction, allowing for faster and more complete surface functionalization.

2.6 SURFACE FUNCTIONALIZATION OF SILICA BEADS WITH BROMO GROUPS

Surface functionalization of silica beads with bromine groups was completed using a previously reported method.[51,52] A 45 mL solution containing silica beads functionalized at the surface with amine groups was allowed to stir at 300 rpm in a RBF equipped with a magnetic stir bar and 0.3 mL of dry pyridine was added. The solution was then put in an ice bath and allowed to cool to 0°C. Once cooled, 0.25 mL of 2-bromoisobutryl was added drop wise. The solution was then allowed to stir for 30 minutes at 0°C. After 30 minutes, the ice bath was removed, and the solution was allowed to stir overnight at room temperature (approximately 14 hours). The following morning, the particles were washed with toluene three times via centrifugation

(Eppendorf 5804R centrifuge) and then three more times with ethanol. The final white pellet was dissolved in a minimal amount of ethanol and then dried in a petri dish on a hot plate set to 50°C for characterization and use for further synthesis.

2.6.1 Approach

The above approach has several key aspects that allow for successful synthesis of this step. Toluene was used for this step because the byproduct of this reaction is a pyridinium salt, which is insoluble in this solvent. As this byproduct falls out of solution, it shifts the equilibrium of the reaction towards the products and allows for better functionalization. However, the salt also sticks to the beads, eventually causing them to fall out of solution as the reaction moves forward and surface functionalization becomes complete. Therefore, it is necessary to wash the particles with ethanol several times to remove the pyridinium salt from the surface of the beads.

2.6.2 Alternative approaches and approach drawbacks

The original procedure called for only washings in toluene to remove excess precursors and then removal of excess solvent via a vacuum oven. However, this method did not remove pyridinium salt formed in the reaction and made proper characterization by NMR impossible since peaks could be observed in the spectrum corresponding to the salt. The above approach solves this issue, but more washing steps means more particles will be lost, since there is always some particle loss during centrifugation.

2.7 ONE-POT SYNTHESIS OF MERCAPTO-SILICA COLLOIDAL SPHERES

This procedure was adapted from a previous report.[53] In a Falcon tube, 29 mL of water, 1 mL of ammonium hydroxide, and 120 μL of MPTMS were combined. This solution was stirred on a vortexer set to the highest setting for 1 minute. The solution was then allowed to sit for 4-5 hours to obtain a milky white color. The solution was then put on the centrifuge (Eppendorf 5804R centrifuge) for 10 minutes at 4000 rpm. The obtained pellet was washed once with 10 mL of 0.01 M NaOH solution and then three times with 10 mL of ethanol.

2.8 SYNTHETIC SCHEME FOR POLYNIPAM COATED SILICA BEADS

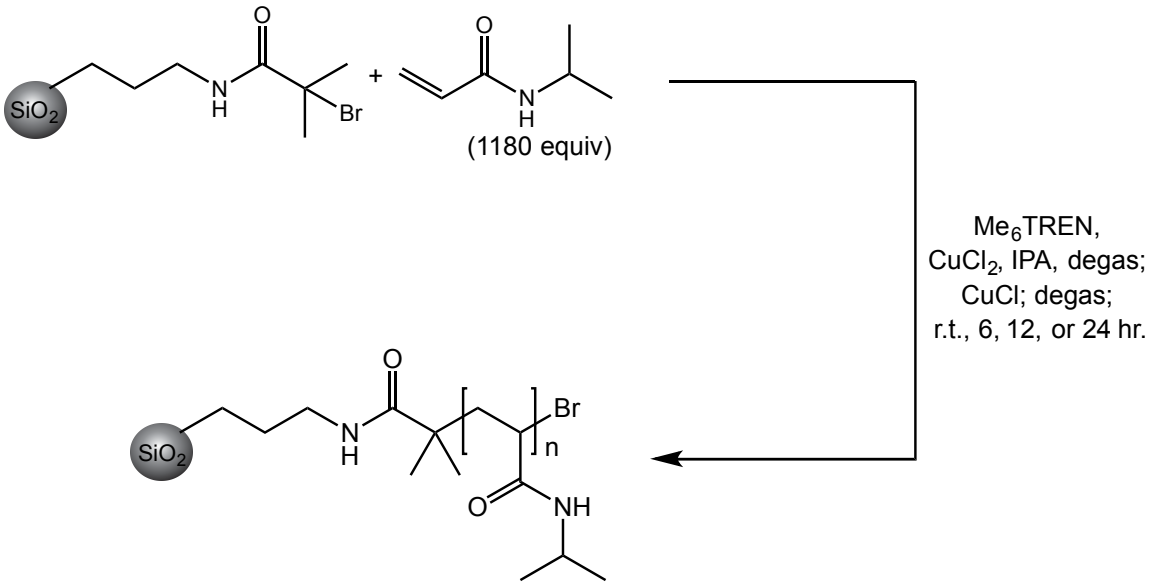

Figure 6. Proposed synthesis of polyNIPAM coated silica beads.

The synthetic goal for the stimuli responsive particles is shown above in **Figure 6** where the solid arrow indicates the reaction conditions. This polymerization reaction should yield silica beads with a temperature responsive shell. Once synthesized, its terminal bromine can be

replaced by an end functional group that is more appropriate for attachment of nanoprisms such as biotin. Then these particles can be combined with prisms that wereligand exchanged with avidin for attachment and bending can be performed.

2.9 SYNTHESIS OF SILICA BEADS COATED IN POLYNIPAM

This procedure was modified from a previously reported synthesis.[51,52] In a typical synthesis, 200 mg 2-bromoisobutyryl functionalized silica nanoparticles, 4 g NIPAM, 1.3 mg $CuCl_2$, 26 mg Me_6TREN (35 μL), and 4 mL IPA were combined in a vial. The vial was sonicated to disperse all of the NIPAM into solution. The solution was transferred to a three neck RBF equipped with a stir bar, and then the vial was washed with an additional 2 mL of IPA, which were then also transferred to the flask. The flask was then attached to a schlenk line via a gas inlet and flushed with nitrogen for 10 minutes. The flask was sealed with rubber septa and was degassed by two freeze-pump-thaw cycles. Then another freeze-pump-thaw cycle was performed, while 15 mg of CuCl was added to the reaction under frozen conditions and positive nitrogen pressure. Once added, two additional freeze-pump-thaw cycles were performed. The reaction was then closed off and allowed to stir for anywhere from 6 to 24 hours depending on the chain length desired. Once the solution had reacted for the desired interval, it was exposed to air and quenched with 6 mL IPA. Water was then added to the solution to form a 70:30 water to IPA mix. This caused the particles to flocculate out of solution and made them easier to spin out by centrifugation (Eppendorf 5804R centrifuge). The particles were spun out at 5,000 rpm for 20 minutes. The resulting pellet was dissolved in ethanol and spun at 2,000 rpm for 5 minutes. This resulted in a brown pellet that consisted of copper byproducts, which was discarded. Water was

added to the remaining solution to form a 70:30 water to ethanol mix and was put on the centrifuge at 5,000 rpm for 20 minutes. The resulting pellet was washed two more times with this water-ethanol solution before being dissolved in a minimal amount of ethanol and allowed to dry in a petri dish on a hot plate set to 50°C overnight.

2.9.1 Approach

The procedure described above allows for sufficient removal of air for the reaction to take place. Air is a known quencher for atom transfer radical polymerization, so it is a significant concern. Based on the results, it was found that this method was sufficient to remove air for the reaction to take place. For purification, it was decided to put the particles into a solvent mixture rather than a pure solvent. In pure solvent, whether it be water or IPA, the particles do not spin out on the centrifuge even at very high speeds due to the very high solubility of polymer. However, in certain solvent mixtures of water and IPA the polymer becomes insoluble, and the particles can be easily spun out on the centrifuge. In addition, time was spent removing excess copper via centrifugation because it was found to interfere with later steps in the synthesis.

2.9.1.1 Clathrate

The key to the purification step in the above synthesis is the formation of a clathrate. A clathrate is simply a lattice that traps or contains molecules.[54] Traditionally, clathrate compounds are polymeric and completely envelop the guest molecule, but in modern usage, clathrates also include host-guest complexes and inclusion compounds.[55] In this example, a host molecule forms a lattice around another guest molecule. The water molecules encapsulate clusters of IPA molecules forming hydrated aggregate structures. The formation of these structures means there

are no solvent molecules available for solvation of the polymer chain, which is necessary for polyNIPAM to be soluble. With no solvation of the polymer chain the collapses to its shrunken state.

2.9.1.2 Co-non-solvency

In the purification of these particles, a interesting phenomenon is observed with solubility. If a particle, molecule, or species is soluble in two solvents it is assumed that it will also be soluble in any mixture of the two. However, here it is observed that this does not hold true. Despite being soluble in both water and IPA, polyNIPAM proves in soluble in a 70:30 water:IPA solution. This is known as co-non-solvency.[55] This is a property typically observed with materials that exhibit an LCST such as polyNIPAM.[56] In these solution mixtures, the solvents form a clathrate and are no longer able to solvate the polymer chain. As this happens, polymer-polymer hydrophobic interactions lead to particle deswelling, and the polymer chain collapses.[57] This effectively lowers the solubility of the particles allowing them to fall out of solution making centrifugation easier.

2.9.2 Alternative approaches and approach drawbacks

The described synthesis could have also been performed in a glove box, which would have greatly eliminated any chance for quenching from air. For the purification, it was also possible to take direct advantage of the LCST and heat the solution containing the particles above 32°C and spin them on the centrifuge. This method leads to less particles being obtained however as the solution cools on the centrifuge, and the particles go back into solution. The

method described above using a schlenk line allows for easier additions, but a higher chance for air contamination.

2.10 ETCHING OF SILICA SPHERES

Polymer free from the surface of the silica nanoparticle was obtained via etching with HF. PolyNIPAM coated silica spheres obtained from the above synthesis (500 mg) were dispersed in 7 mL of water resulting in a milky white solution. 7 mL of a 14% v/v HF stock solution was added to the polyNIPAM coated silica bead solution. If aggregation occurred, which was the case for longer polymer chains, then the solution was diluted and mixed to disperse the particles again. This solution was allowed to sit overnight, and the resulting solution was completely clear. The solution was transferred to molecular weight cut off filters (Millipore 10k cut-off) and centrifuged. Three washings with water followed this in the molecular weight cut off filters. The free polymer now trapped on the cut off filters was then dissolved in a minimal amount of water, and transferred to a petri dish, and dried on a hot plate set to 50°C for further characterization. Evidence of the polymer could be seen in the water, which appeared to have soap suds. *Caution: HF is highly dangerous substance and requires proper personal protective equipment including the use of silver shield gloves. HF should be handled in a fume hood only, and special care should be taken not to get any on skin or clothing.*

2.11 SYNTHETIC SCHEME FOR FUNCTIONALIZATION OF POLYMER TERMINAL GROUP WITH BIOTIN

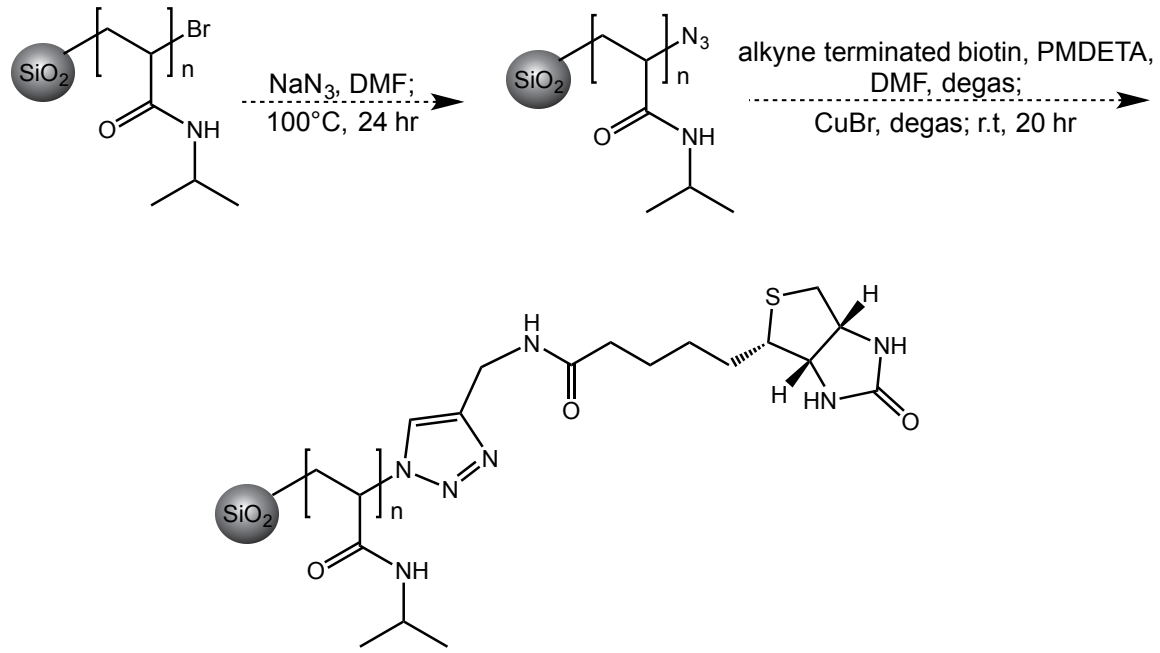

Figure 7. Proposed scheme to terminate the polymer chains in the molecule biotin.

A proposed scheme for the terminal group functionalization with biotin is shown above in **Figure 7**. The dotted arrows indicate that these reactions have not been completed yet, but the first step has been attempted, and the procedure is outlined below. The above scheme will be used in future experiments once the terminal functionality of bromine can be maintained following the initial polymerization (*vide infra*).

2.12 ATTEMPTED SYNTHESIS OF POLYNIPAM COATED SILICA BEADS TERMINATED WITH AZIDE

This is a modified procedure of a previous synthesis.[52] First, polyNIPAM coated silica beads were transferred to dialysis tubes (procedure described previously) to remove excess copper. 1 g of polyNIPAM coated silica beads and 9 mL DMF were combined in a 100 mL RBF equipped with a magnetic stir bar. The RBF was sonicated to dissolve all of the particles, and then 0.1 g NaN_3 was added to the solution. The solution was then placed in an oil bath and covered with aluminum foil to protect it from light. The solution was then heated to 100°C and set to stir for 24 hours. After 24 hours, the solution was taken off heat, and water was added to form a 70:30 water to DMF mix. This solution was centrifuged at 5,000 rpm for 20 minutes and washed three times with a 70:30 water to ethanol mix as with the regular polyNIPAM coated silica beads. The final pellet was dissolved in a minimal amount of ethanol and put in a petri dish on a hot plate set to 50°C to dry.

2.13 SYNTHETIC SCHEME FOR BIOTIN TERMINATED IN AN ALKYNE

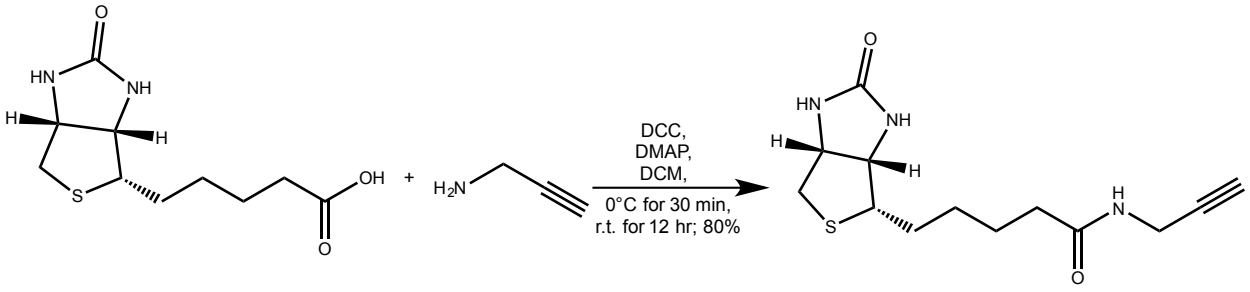

Figure 8. Proposed scheme showing the coupling reaction of biotin with propargylamine.

The completed synthesis of the biotin molecule terminated in an alkyne group for "click" chemistry with the azide to be put on the end of the polymer is shown above in **Figure 8**. This coupling reaction will allow for the addition of biotin onto the end of the polymer chain.

2.14 SYNTHESIS OF ALKYNE TERMINATED BIOTIN

Alkyne terminated biotin was prepared using a modified synthesis.[52,58] 3.03 g biotin, 3.0 g DCC, 0.18 g DMAP, and 50 mL dry CH_2Cl_2 were combined in a 250 mL RBF equipped with a magnetic stir bar. The solution was cooled to 0°C via an ice bath and set to stir. A solution containing 0.80 g propargylamine dissolved in 10 mL dry CH_2Cl_2 was then added drop wise. This reaction was allowed to stir for 12 hours at room temperature. The solvent was removed via a rotary evaporator and purified via column chromatography in a 65:25:10 chloroform:methanol:water mixture as effluent. (80%) **^{1}H NMR** (400 MHz d-DMSO) δ= 8.217 (t, 7.8 Hz, 0.9H), 6.420 (s, 1.1H), 6.348 (s, 1.0H), 5.568 (d, 8.8Hz, 2.1H), 4.300 (t, 7.8 Hz, 1.1H), 4.131 (t, 7.8 Hz, 1.0H), 3.831 (s, 0.9H) 3.100 (t, 7.8 Hz, 1.0H), 2.823 (t, 7.8 Hz, 1.1H), 2.202 (t, 7.8 Hz, 1.9H), 2.078 (t, 7.8 Hz, 1.1H), 1.8-1.5 (m, 6.6H).

3.0 RESULTS AND DISCUSSION

3.1 PRELIMINARY EXPERIMENTS TO DETERMINE THERMAL FLUCTUATION

In order to determine the optimal size of the stimuli responsive bead template, studies must first be conducted to determine the thermal fluctuation of the anisotropic gold nanoparticles. The nanoparticles in solution should have some thermal fluctuation that will allow them to attach to a curved surface. The initial studies help to determine the bead size and the attraction type that will be used in the desired system we are trying to create. In these studies, bead size will be varied to determine how small a bead to which gold nanoparticles will attach conformally to. This size will depend on the inherent thermal fluctuations of the gold nanoparticle as well as the strength of the attraction between the gold nanoparticle and the template surface. The first step in these studies will be to synthesize silica beads of different sizes while maintaining monodispersity. Once there is control over size, the surface can be functionalized in different ways for different interaction types, and the functionalized silica beads can be combined with the gold nanoparticles. Then degree of bending can be calculated using the method below.

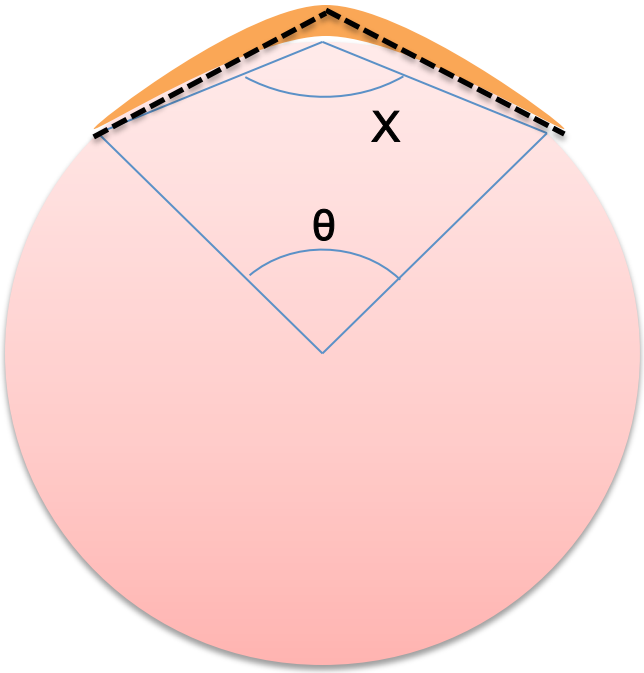

Figure 9. Diagram showing a prism conformally attached to a silica bead and the associated angle of bending

Angle θ can be determined using L, the length of the anisotropic nanoparticle, and D, the diameter of the silica bead. This yields the equation:

$$\theta = \frac{Lx360}{\pi D}$$

Angle X can then be determined using θ and geometry giving the equation:

$$X = \frac{360 - \theta}{2}$$

Finally, the angle of bending of the anisotropic nanoparticle is simply the value X taken from 180 degrees, which is associated with an unbent particle yielding:

$$Degree\ of\ Bending = 180 - X$$

3.1.1 Silica Bead Templates

Silica beads were synthesized at various sizes. These particles were characterized by TEM to determine particle size and polydispersity. A representative images is shown below.

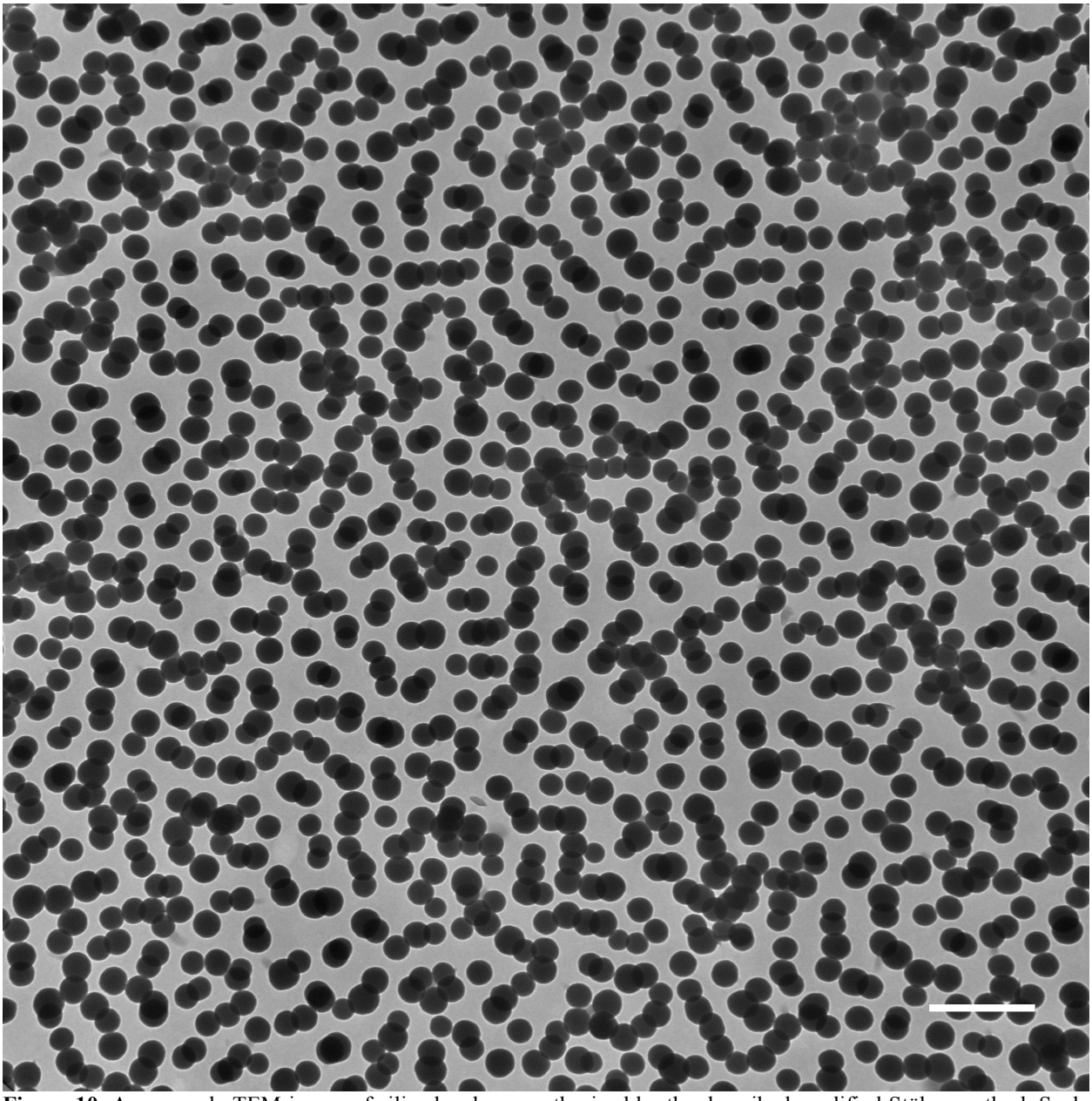

Figure 10. An example TEM image of silica beads as synthesized by the described modified Stöber method. Scale bar is 500 nm.

Average population sizes were then determined using ImageJ 1.47d (National Institutes of Health, USA). For each size, at least 200 particles were measured to get an accurate value of the population distribution. Below is a graph showing the different sizes synthesized and error bars which correspond to the standard deviation in the sizes.

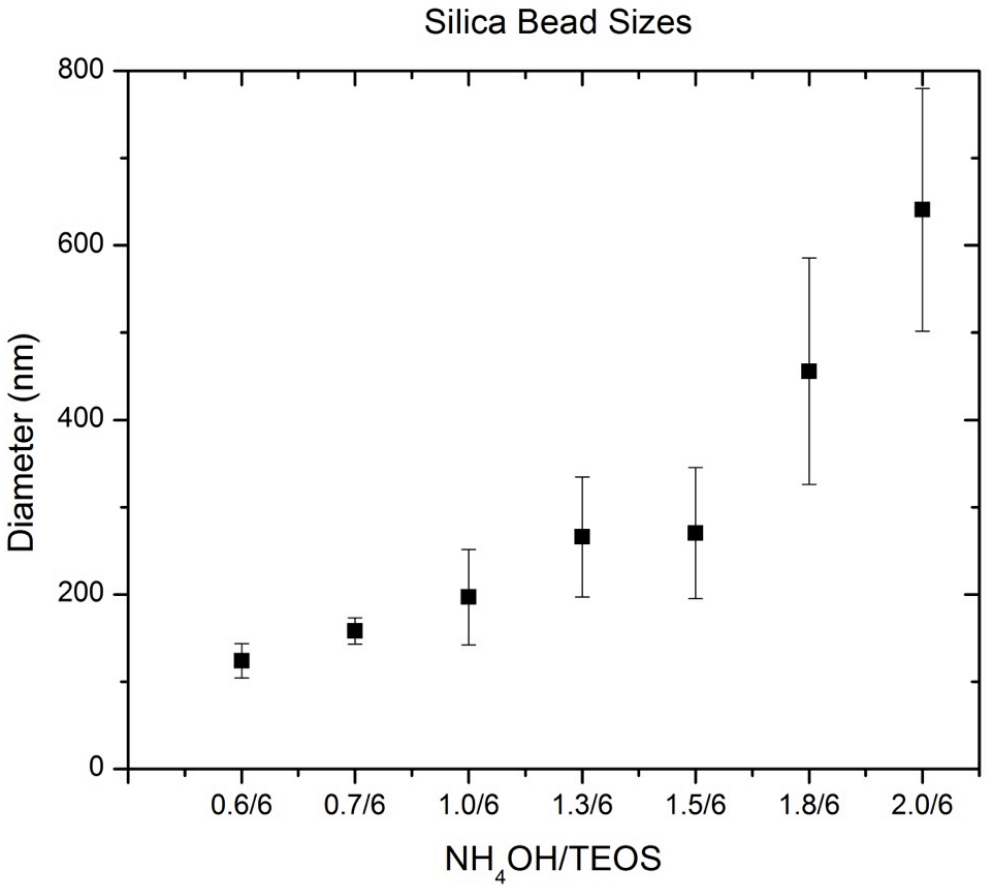

Figure 11. Graph showing the different sizes of as-synthesized silica beads and their corresponding population distributions shown as error bars.

3.1.2 Silica beads surface functionalized with amine groups

For studies, performed to determine the effectiveness of electrostatic attraction, first amine beads were first synthesized and characterized. Zeta potential measurements before and

after functionalization showed a significant change in the surface charge of the silica beads. Prior to functionalization, zeta potential was determined to be -50.2 ± 3.4 mV. After functionalization, the zeta potential changes drastically to 45.4 ± 4.4 mV. This change in surface charge shows that there has been a distinct change in the functional groups at the surface. In addition, this functionalization was confirmed using the molecule ninhydrin (2,2-Dihydroxyindane-1,3-dione). Ninhydrin reacts with amine groups in solution. In the absence of amine groups, it appears yellow in solution. However, in the presence of amines, ninhydrin changes to a deep blue or purple color as it reacts with the amine groups. The bare silica beads were tested first, and only the yellow color is seen. However, when ninhydrin is in solution with silica beads that have been surface functionalized with amine groups, the transition to the characteristic blue color is seen. This can also be monitored using UV-vis-NIR spectroscopy, and this is shown in the spectra below.

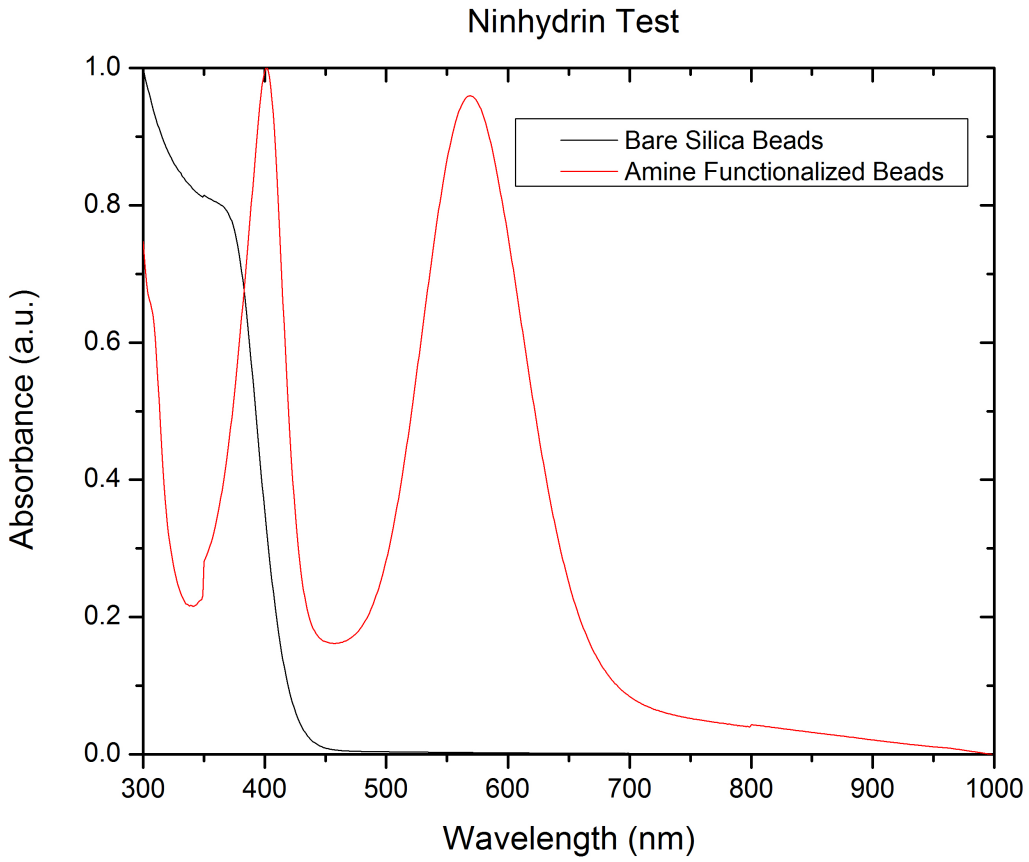

Figure 12. UV-Vis Spectra of silica beads with ninhydrin both before and after surface functionalization with amine groups.

3.1.3 Bending of nanoprisms using electrostatic interactions

Gold nanoprisms functionalized with PVP were put into solution with silica beads surface functionalized with amine groups. Again, due to the negative charge of the PVP and the positive charge of the amine groups, there should be an electrostatic attraction between the silica beads and the nanoprisms. The results are shown in the images below.

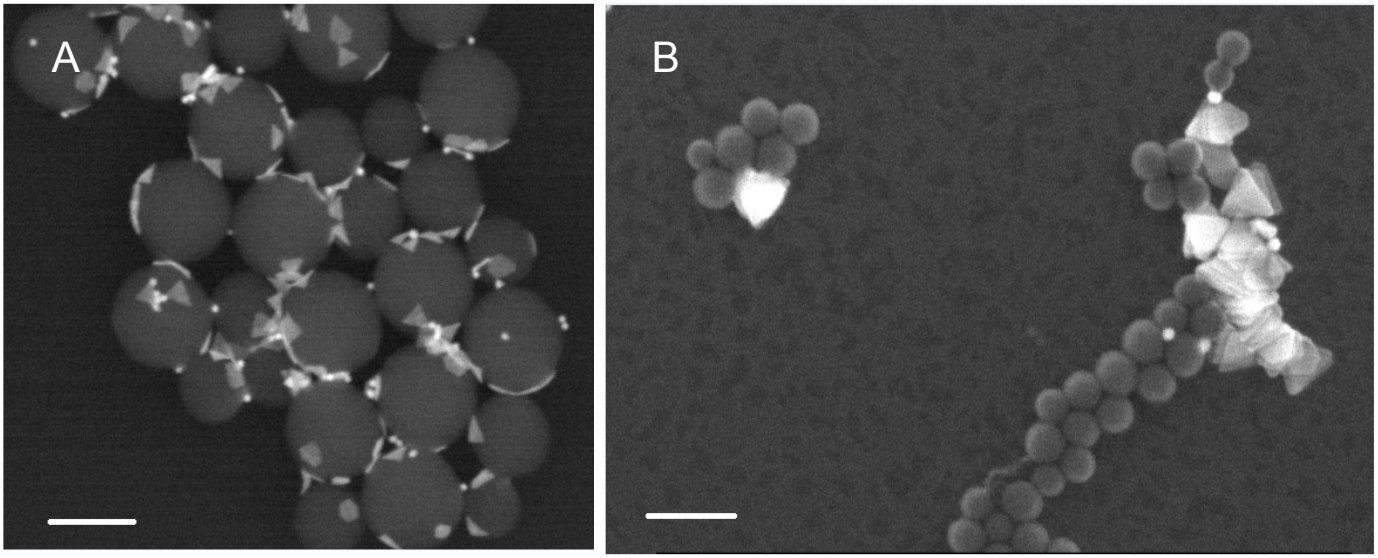

Figure 13. SEM images of PVP coated gold nanoprisms mixed with silica beads of A) 483 nm, scale bar is 500 nm and B) 126 nm scale bar is 200 nm.

It can be seen that with beads with an average size of 483 nm, conformal attachment of the gold nanoprisms and slight bending occurs. However, it can be seen with beads of an average size of 126 nm that the beads and nanoprisms stay separate, and bending does not occur. Lastly, nanoprisms coated in PSS were mixed silica beads surface functionalized with amine groups. PSS has a stronger negative charge associated with it, so a stronger electrostatic interaction should result. These prisms were mixed with smaller beads than the PVP coated prisms where bending was observed. Below is a representative SEM image of this experiment.

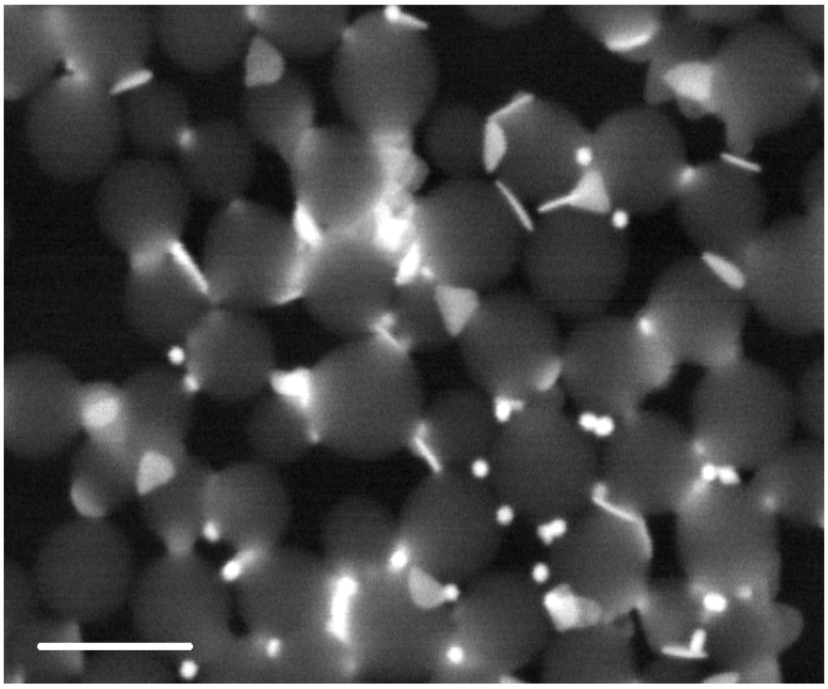

Figure 14. SEM image of PSS coated nanoprisms mixed with amine functionalized silica beads of size 306 nm. Scale bar is 500 nm.

As can be seen in this image, prisms do attach but not conformally to beads of size 306 nm, which indicates that no bending occurs. The bending from the PVP coated prisms with the large silica beads can be calculated using the method discussed earlier, meaning that the smallest bead that will yield conformal attachment using an electrostatic attachment is 483 nm. This gives a degree of bending equal to 11.9 using the previously described method to calculate degree of bending.

3.1.4 Bending of nanoprisms using a gold thiol interaction

Gold nanoprisms were put in solution with silica beads surface functionalized with thiol groups. This interaction should prove to be much stronger than an electrostatic interaction, which is on the order of 10-20 kcal/mol depending on the strength of the charge on each species.[59] A gold thiol interaction should be on the order of 50-70 kcal/mol (for a self assembled monolayer) depending on the chain length of the alkane thiol attached to the surface.[60] This stronger

interaction may allow for conformal attachment of gold nanoprisms to smaller silica beads. Smaller silica beads have a higher radius of curvature and therefore a greater degree of bending. Shown below is a SEM of the results of this experiment.

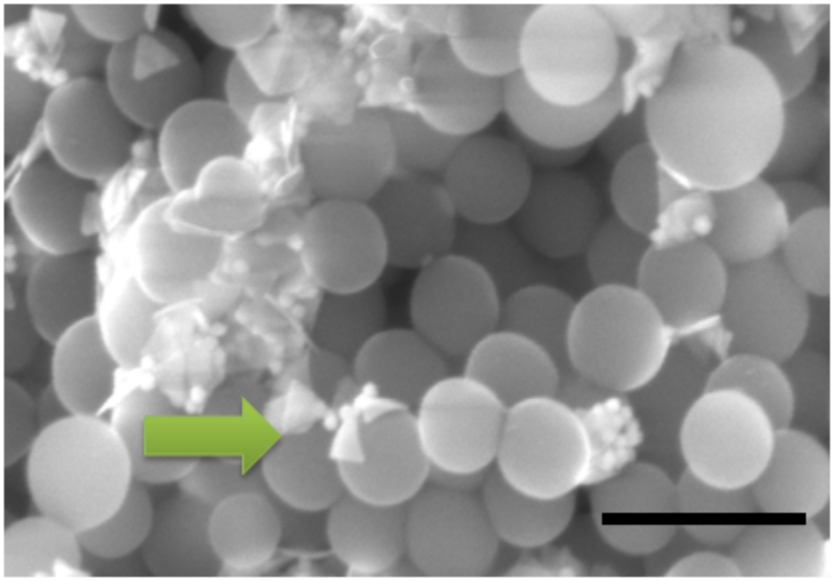

Figure 15. SEM image of thiol surface functionalized silica beads mixed with gold nanoprisms. Scale bar is 500 nm.

Above the arrow points out that conformal attachment was achieved. Using the method to calculate bending gives a degree of bending equal to 23.9. Thus, through a stronger interaction, it is possible to attach prisms to smaller beads and get a higher degree of bending.

3.2 SYNTHESIS OF POLYNIPAM COATED SILICA BEADS

The above preliminary studies have given some insight into the thermal fluctuations associated with anisotropic gold nanoparticles. These studies show the smallest size of beads that can be used for prism attachment, given a certain interaction. Now, this information can be used to build the stimuli responsive bead template. First, silica beads will be surface functionalized with bromine groups, which can then be used as initiators for the polymerization,

and then the polymer terminal group can be modified to biotin. Finally, Gold nanoprisms can be ligand exchanged with thiol terminated avidin and bending can be attempted.

3.2.1 Silica beads surface functionalized with bromine groups

For ATRP, it is necessary to have a halide group as the initiator. Therefore, it is necessary to modify our silica bead template, so that the surface is functionalized with bromine groups. This will allow for chain growth directly from the surface of the silica beads, resulting in particles with a core-shell morphology. To functionalize the surface with bromine groups, silica beads surface functionalized with amine groups were reacted following the scheme in **Figure 16**. Solid-state ^{13}C NMR was used to evaluate the success of this reaction.

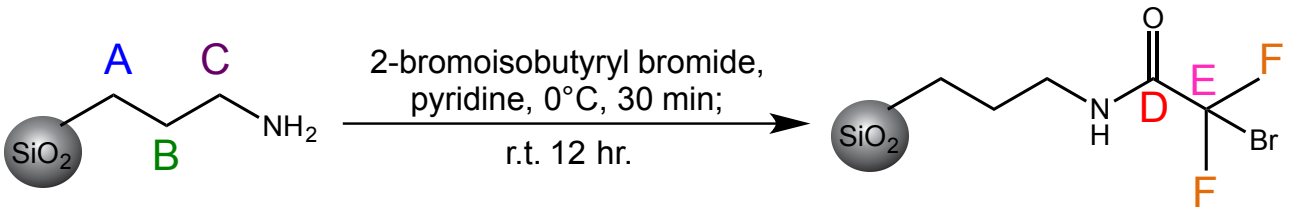

Figure 16. Scheme showing the synthesis of silica beads surface functionalized with bromine, with carbons labeled so they correspond to peaks in the ^{13}C NMR below.

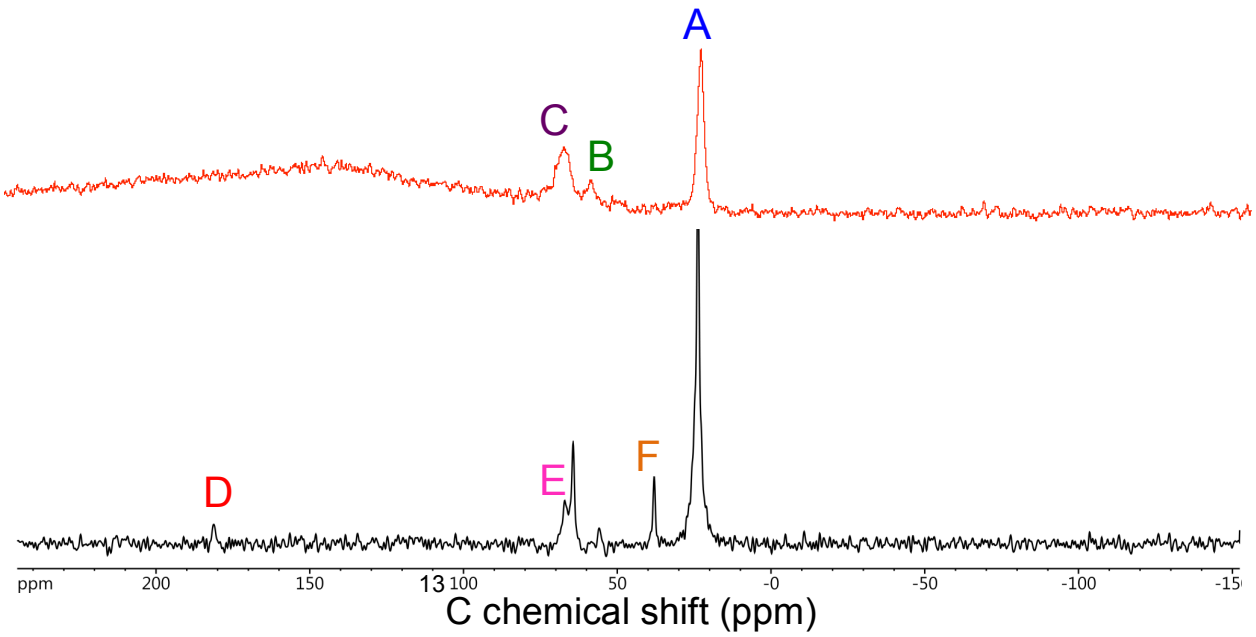

Figure 17. ^{13}C NMR of silica beads surface functionalized with amine groups (top) and surface functionalized bromine groups (bottom). Peaks are labeled so they correspond to the scheme above.

The above spectra show the ^{13}C-NMR of the precursor amine functionalized silica beads and the resulting bromine functionalized silica beads. It can be seen that the carbon peaks associated with the amine functionalized silica beads remain in the bromine functionalized silica beads. However, three new peaks appear which correspond to the carbonyl carbon, the carbon with the bromine attached to it, and the methyl carbons. This proves that functionalization has occurred. In addition, the peaks correspond well to a ^{13}C-NMR spectrum of the 2-bromoisobutryl bromide.

3.2.2 PolyNIPAM coated silica beads

PolyNIPAM was grown from the bromine functionalized silica beads using ATRP. The reaction time was varied to give several different sizes of particles. These particles were synthesized at 6, 12, and 24 hours. The sizes of the particles could then be determined using DLS measurements. At 6, 12, and 24 hours the beads grow to 331 ± 2.95 nm, 388 ± 4.21 nm, and 470 ± 7.71 nm, respectively from the bromine functionalized silica beads of size 180 ± 1.75 nm. In addition, the temperature dependence of these sizes can be seen on DLS by slowly raising the temperature and taking size measurements at every increased degree of temperature.

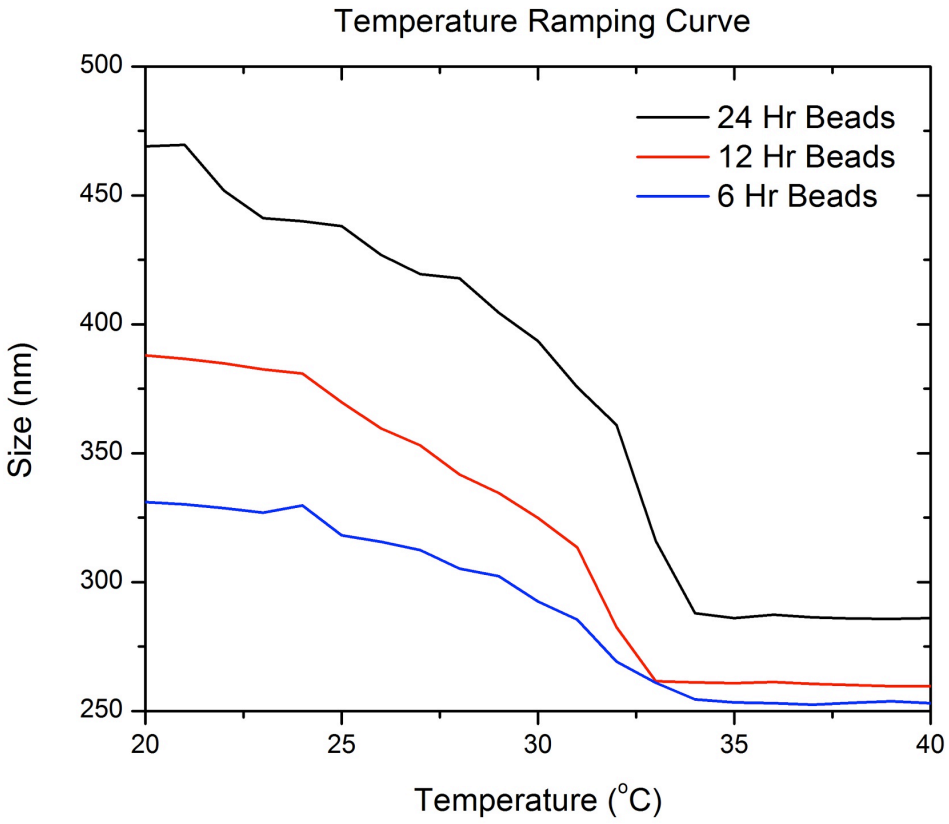

Figure 18. Graph showing size vs. temperature of three different sizes of polyNIPAM coated beads: 6, 12, and 24 hour.

As observed from the above graph, the particle size significantly decreases around and above 32°C, whereas the bromine functionalized silica bead precursor shows relatively no change in size. This temperature size dependence suggests that the polymerization was successful and stimuli responsive nanoparticles have been synthesized. The first derivative of the temperature dependence can also be taken and used to determine the temperature at which this size change happens which should be the minimum of the graph. This shows transition temperature for 6, 12, and 24 hour happening at 32.4 ± 0.3°C, 32.3 ± 0.1°C, and 32.5 ± 0.2°C respectively. In addition, by taking the full width at half max of this minimum, how quickly this temperature change happens can be determined (meaning not the rate of the shrinking, but rather over how many degrees this change is happening) The table below shows a summary of the DLS data.

Table 1. Table summarizing data collected via DLS

Parameter	6 hour	12 hour	24 hour
Size by DLS (nm)	331 ± 2.95	388 ± 4.21	470 ± 7.71
Transition Temperature (°C)	32.4 ± 0.3	32.3 ± 0.1	32.5 ± 0.2
Full Width at Half Min (°C)	3.18 ± 0.5	2.18 ± 0.2	2.45 ± 0.3

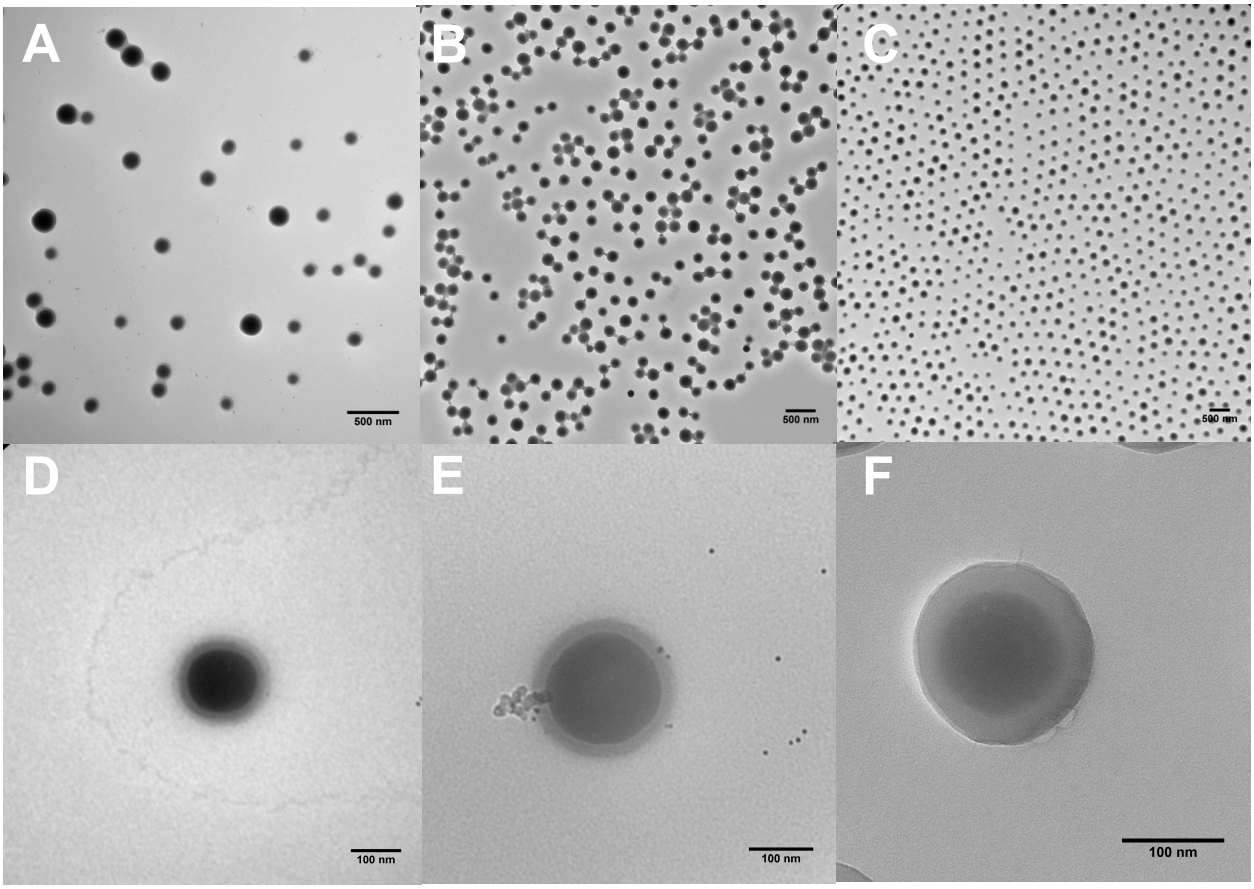

Figure 19. TEM images of particles allowed to react for different times. A and D are a 6 hour reaction. B and E are a 12 hour reaction. C and F are a 24 hour reaction. In addition, A, B, and C show populations of particles and D, E, and F show single particle morphology.

Next, TEM was used to confirm the core-shell morphology of these particles. In TEM, light materials such as polymers appear more transparent since carbon has a lower atomic number and therefore more electrons can be transmitted through the material.[61] Thus, it is expected that our silica core should be darker surrounded by a lighter shell of polymer. Again, particles reacted for 6, 12, and 24 hours were characterized and images are shown above. It is clear from the above images that as reaction time is increased so are shell thicknesses. This agrees with the DLS data since bigger particles were observed with longer reaction time. The

shell thicknesses for the 6, 12, and 24 hour beads were 14.95 ± 2.03 nm, 25.02 ± 1.95 nm, and 35.64 ± 1.54 nm respectively.

Now that growth of the polymer from the silica bead has been confirmed, the polymer itself also needs to be characterized. For proper characterization of the polymer, it is necessary to have free polymer not bound to a silica bead. HF was therefore used to etch away the silica bead leaving only the free polyNIPAM. After etching took place, free polymer could be analyzed by GPC to determine number-average molecular weight (M_n), weight-average molecular weight (M_w), degree of polymerization (DP), and polydispersity (PDI). M_n, M_w, and PDI are given by the GPC, but the equations to solve for them are listed below, where M_i is the molecular weight of a given chain and N_i is the number of chains of a given length.

$$M_n = \frac{\sum M_i N_i}{\sum Ni} \qquad M_w = \frac{\sum M_i^2 N_i}{\sum M_i N_i} \qquad PDI = \frac{M_w}{M_n}$$

In addition, degree of polymerization can be determined by dividing the M_n by the molecular weight of the monomer unit, which for NIPAM is 113.16 g/mol. A representative graph of one of the GPC measurements is shown below along with a table of the GPC data for 6, 12, and 24 hour polyNIPAM coated silica beads.

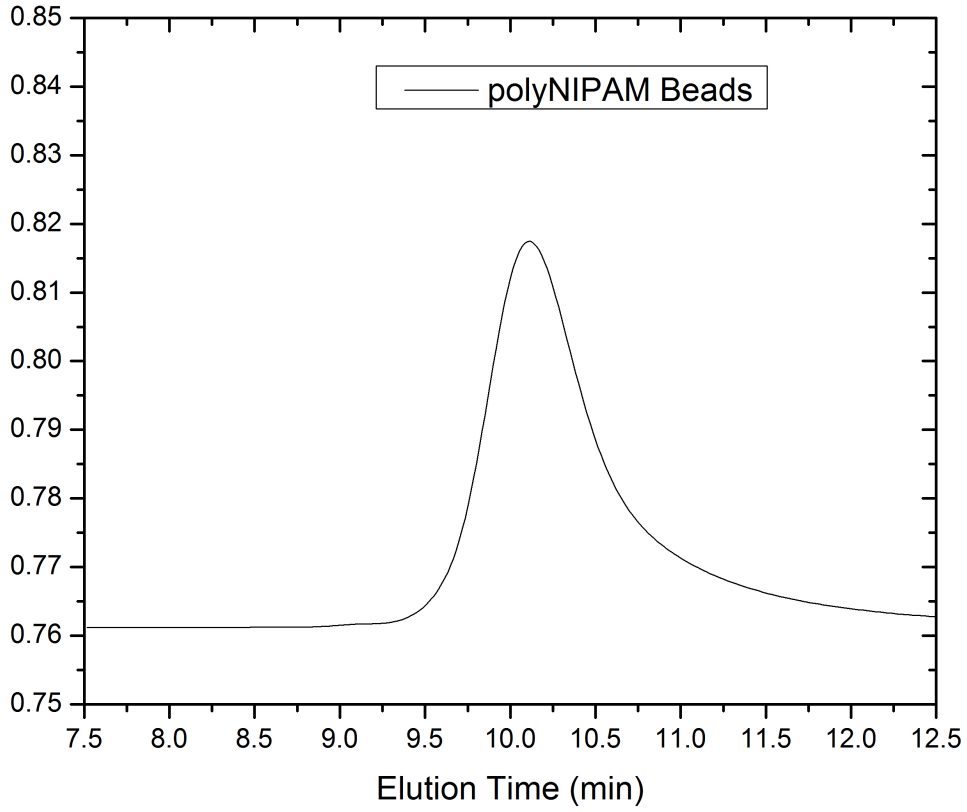

Figure 20. Example GPC graph of polyNIPAM beads

Table 2. Table summarizing data collected by GPC

Parameter	6 hour	12 hour	24 hour
M_n (g/mol)	24,622	31,021	40,741
M_w (g/mol)	29,546	35,367	45,853
DP (monomer units)	218	274	360
PDI	1.20	1.14	1.12

3.3 ATTEMPTED CONVERSION OF THE TERMINAL GROUP OF THE POLYMER

3.3.1 Attempted azide terminated polyNIPAM coated silica beads

PolyNIPAM coated silica beads were believed to be terminated in bromine groups, which should allow for functionalization with azide. An azide at the end of the chain would allow for click chemistry with a modified biotin molecule. Biotin at the surface would allow for attachment of gold nanoprisms and bending could be performed. Initially, results seemed to indicate that the azide functionalization was successful. PolyNIPAM coated silica both before and after functionalization was analyzed by FTIR, and the spectrum is shown below. The peaks characteristic to polyNIPAM appeared in the spectrum both before and after functionalization. These characteristic peaks are the amide I band (1650 cm^{-1}, C=O stretching) and the amide II band (1550 cm^{-1}, N-H stretching). However, a new peak at approximately 1900 cm^{-1} appears in the spectrum post functionalization. This peak is where an azide stretch would be expectedto appear, so it seems to confirm that an azide is terminating the polyNIPAM chain.

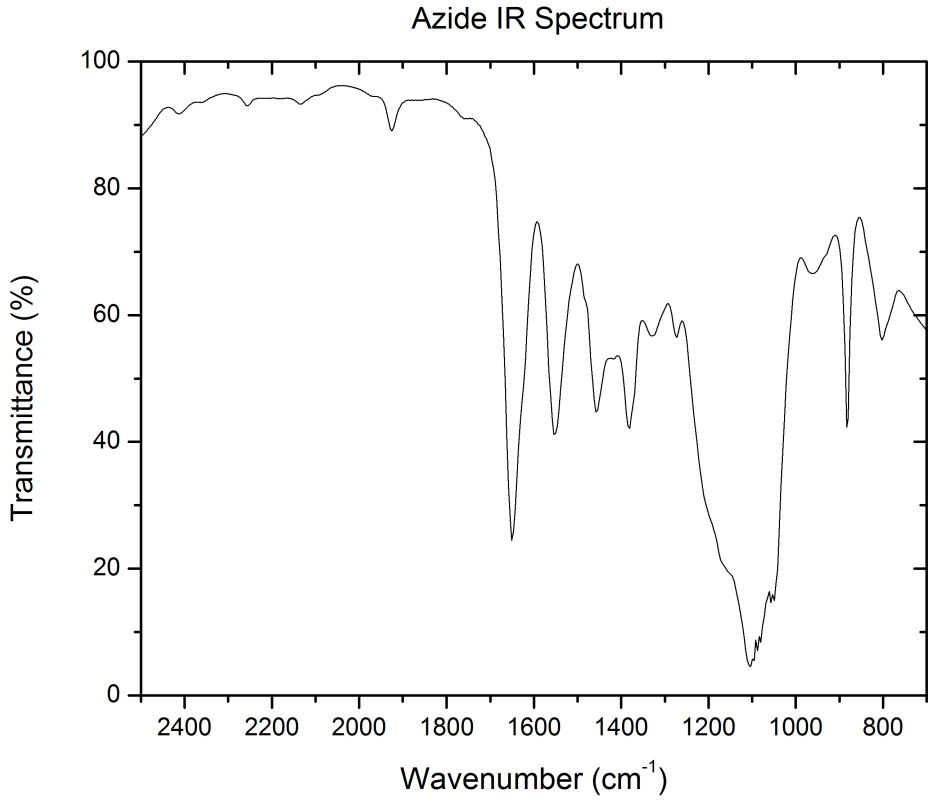

Figure 21. IR Spectrum of polyNIPAM coated silica beads after attempted functionalization with azide.

Azide termination seems to be confirmed by IR. However, more characterization of these particles to is necessary ensure that the azide is present for the next step of the reaction. As a second way to characterize this functionalization, MALDI-TOF was used. MALDI is a sensitive technique that should allow for precise determination of molecular weights. Here we will use it to determine if there is a change in the terminal group of the polymer. Bromine has a known 50:50 natural abundance of its ^{79}Br and ^{81}Br isotopes. Therefore, a sample containing bromine should have a doublet associated with it. Thus, if a polymer is run before functionalization, a doublet should be observed in the spectrum, where as post functionalization, no doublet should be observed. Again, the silica cores were etched from the polymer chains using HF. However, when samples of the polyNIPAM beads pre-functionalization were analyzed by the MALDI-TOF, a doublet was not observed as shown in **Figure 22**.

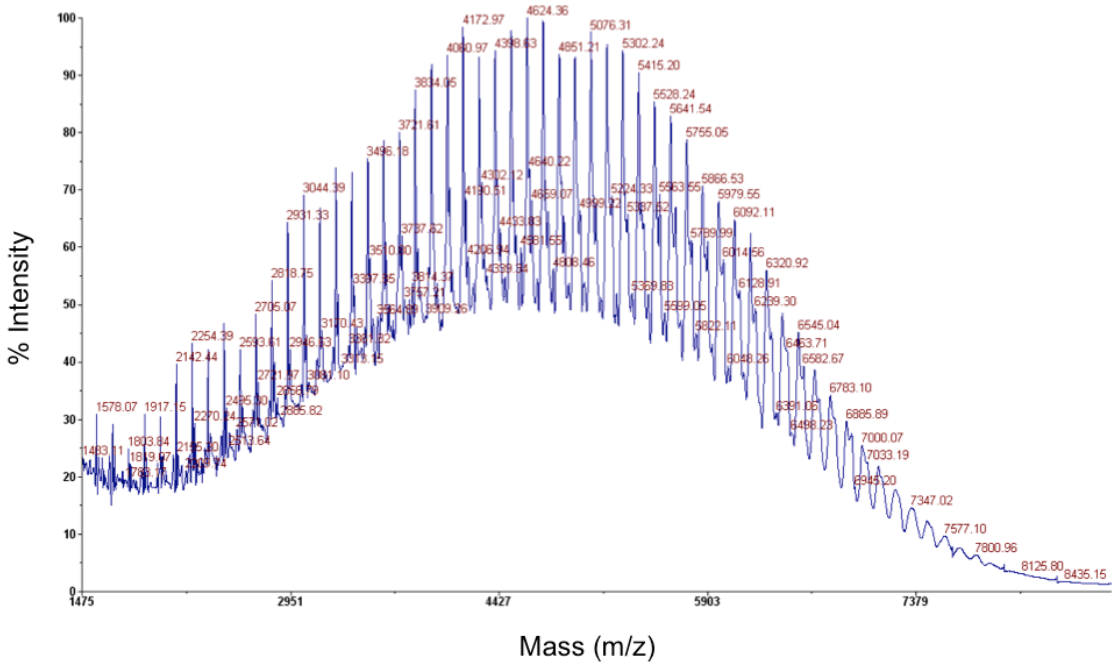

Figure 22. MADLI-TOF spectrum of as-synthesized polyNIPAM coated silica beads

This indicates that not only was the azide functionalization not successful, but the majority of the polymer chains were not terminated in bromine groups. When looking into the literature, it was found that the copper catalyst in its +2 oxidation state causes a β-hydride elimination reaction.[62,63] This means that the terminus of the polymer is not easily changed and these synthetic methods will need to be modified.

The data from the MALDI experiments disagrees with that from the FTIR data. However, upon closer inspection, this discrepancy can be resolved. After the azide functionalization, the solution containing the polyNIPAM beads turns a bright orange color. This orange color results from the azide reacting with residual copper from the polymerization forming a copper azide. Even though special care was taken to remove excess copper, it still is present, as is apparent with the resulting IR spectra and the azide peak that appears on it. Therefore, for future experiments copper must be completely removed from polyNIPAM coated silica beads. To

accomplish this, the beads were put in dialysis tubes for 3 weeks to remove any residual copper. When this was done and the azide reaction was attempted again, no orange color resulted and no peak is observed in the IR.

4.0 CONCLUSIONS AND FUTURE WORK

4.1 CONCLUSIONS

The initial studies on bead size, attraction type, and gold nanoparticle thermal fluctuations have been completed and have resulted in insight into how much a gold nanoprism can be expected to conform to a curved surface. These preliminary studies were key in determining bead size and attraction type. In addition, stimuli responsive bead templates have been synthesized and fully characterized. A silica core with a polyNIPAM shell has been synthesized and this morphology has been shown using TEM. In addition, size and size temperature dependence have been shown using DLS experiments. These experiments showed that the particles exhibit polyNIPAM's transition temperature at 32°C. The polymer has also been removed from the surface of the silica bead for studies using GPC and MALDI. GPC data gave molecular weight, polydispersity, and degree of polymerization. MALDI was used to determine chain termination. It was determined that using this synthesis, the majority of polymer chains are not terminated in bromine.

The lack of a high degree of bromine termination means further attempts to change the terminal group to a biotin will prove difficult. For this reason, conventional ATRP has been determined to not be suitable for the needs of this project. The next set of experiments will require modification of ATRP in a way that will allow for a higher percentage of polymer chains

terminated in bromine. Once bromine is at the end of the majority of chains, the azide functionalization can be attempted. This azide group can then be used for click chemistry with a biotin molecule terminated in a triple bond. Finally, the stimuli responsive bead template will be ready to perform mechanical deformation on gold nanoprisms.

4.2 NEXT SET OF EXPERIMENTS

Although the stimuli responsive bead templates have been synthesized, more work on changing the terminal functionality needs to be done. Rather than changing to a new polymerization method entirely, it is possible to slightly modify the synthesis with a reducing agent. The Matyjaszewski group has been able to increase the number of chains terminated in bromine in ATRP syntheses from 48% to 87-92%[64] through the use of a reducing agent such as Tin(II) 2-ethylhexanoate. This method is known as ARGET (Activator ReGenerated by Electron Transfer) ATRP. Using this reducing agent they recycle their copper catalyst from its +2 oxidation state to its +1 oxidation state, greatly decreasing the chances of β-hydride elimination. In addition, less catalyst needs to be used in this type of synthesis, so the odds of termination are further reduced. Thus, this idea can also be applied to the system being. The Matyjaszewski group has also been able to determine the percent termination using ^{1}H NMR, so it will also be possible to quantify the percentage chains terminated in bromine just as they have.[64-65]

After the completion of the modified polyNIPAM synthesis, the azide reaction can be attempted again, and functionalizing the chain ends with bromine should prove successful. From there, click chemistry can be used to add a modified biotin molecule, which has already been

synthesized, purified, and characterized by NMR, to the chain end. The NMR spectrum of the modified biotin molecule is shown below.

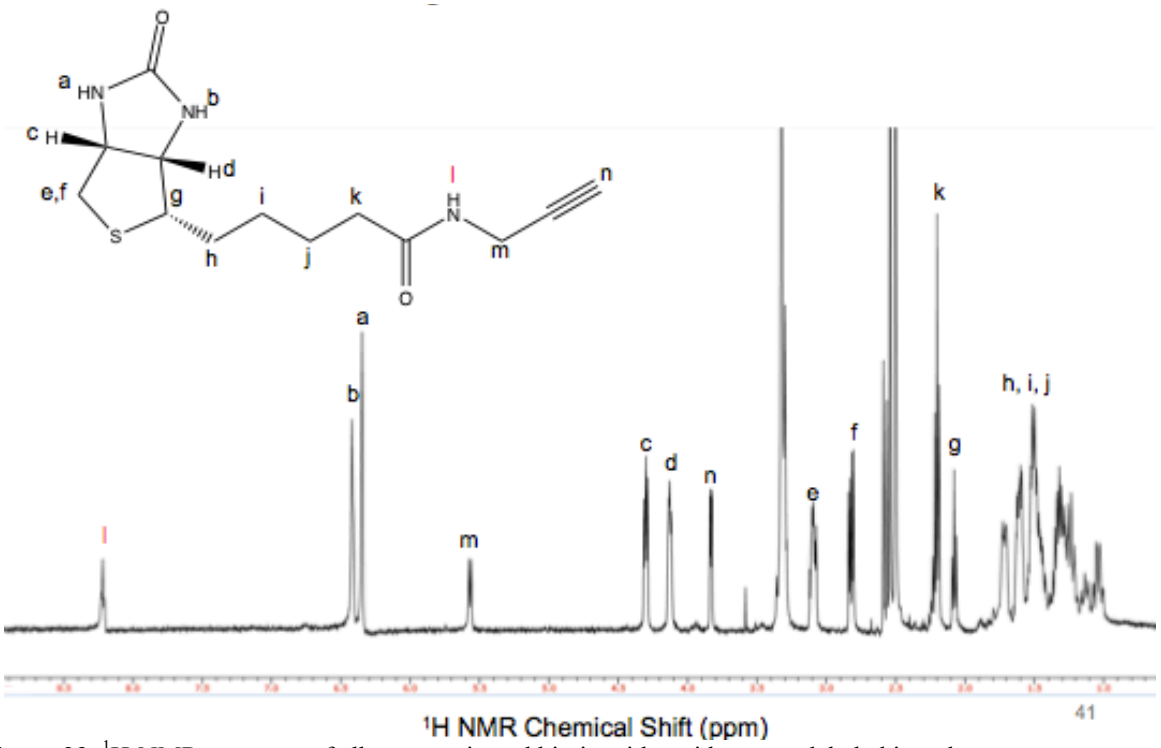

Figure 23. [1]H-NMR spectrum of alkyne terminated biotin with amide proton labeled in red.

With the particles completed and chain ends functionalized with biotin, gold nanoprisms can then be ligand exchanged with thiol terminated avidin molecules by simply stirring overnight in solution with the thiol terminated avidin. Finally, these nanoprisms can be added to our stimuli responsive templates and mechanical deformation can be performed.

4.3 FUTURE WORK

Bending of nanoparticles should result in a change in the overall physical properties of the nanoparticle and an increased chemical reactivity at the defect site. In the case of gold anisotropic nanoparticles, we should be able to monitor a change in the LSPR based on

temperature using UV-Vis-NIR Spectrometry. This will show an obvious change in the physical properties of the material. In addition, the defect site should have an increased reactivity compared to the rest of the particle, since it is already known that defect sites and crystal facet edges are more chemically reactive than the bulk.[20] This allows for the production of nanoparticles with multiple functionalities. This defect site can be used as a focal point for rapid ligand exchange and then used to couple the gold nanoprism to another nanoparticle such as one that exhibits magnetic properties, such as pseudo-spherical iron oxide nanoparticles. This could result in in magnetically addressable plasmonic nanoparticles for cancer ablation.

This idea of using mechanical deformation to change the chemical reactivity of nanoparticles can then be expanded to other nanoparticles. By bending gold nanorods, the defect site created could be used as a nucleation site for polymer growth. From the defect site poly(pyrrole), which is known to actuate upon electrical stimulationcould be grown.[66] This could then be used as an artificial cilia. In addition, other hybrid materials can be imagined; this method could be used to bend CdSe nanorods and then grow another material like a polymer such as poly(thiophene) or an inorganic material such as silver at the defect site.

BIBLIOGRAPHY

1. Xia, Y.; Xiong, Y. J.; Lim, B.; Skrabalak, S. E., *Angew. Chem.* **2009,** *121*, 62.

2. Xia, Y.; Xiong, Y. J.; Lim, B.; Skrabalak, S. E., Shape-Controlled SYnthesis of Metal Nanocrystals: Simple Chemistry Meets Complex Physics. *Angew. Chem.* **2009,** *48*, 60.

3. Burda, C.; Chen, X. B.; Narayanan, R.; Chem., M. A. E.-S.; Rev. 2005, 1025., Chemistry and Properties of Nanocrystals of Different Shapes. *Chem. Rev.* **2005,** *105*, 1025.

4. C. Xue, C. A.; Mirkin, A., pH-Switchable Silver Nanoprism Growth Pathways. *Angew. Chem.* **2007,** *46* (12), 2036-2038.

5. Nikoobakht, B.; El-Sayed, M. A., Preparation and Growth Mechanism of Gold Nanorods (NRs) Using Seed-Mediated Growth Method. *Chem. Mater.* **2003,** *15* (10), 1957-1962.

6. Millstone, J. E.; Hurst, S. J.; Metraux, G. S.; Cutler, J. I.; Mirkin, C. A., Au and Ag Nanoprisms. *Small* **2009,** *5*, 646.

7. Straney, P. J.; Andolina, C. M.; Millstone, J. E., Seedless Initiation as an Efficient, Sustainable Route to Anisotropic Gold Nanoparticles. *Langmuir* **2013,** *29* (13), 4396-4403.

8. Andolina, C. M.; Dewar, A. C.; Smith, A. M.; Marbella, L. E.; Millstone, J. E., Photoluminescent Gold–Copper Nanoparticle Alloys with Composition-Tunable Near-Infrared Emission. *J. Am. Chem. Soc.* **2013,** *135*, 5266.

9. Driskell, J. D.; Lipert, R. J.; Porter, M. D., Labeled Gold Nanoparticles Immobilized at Smooth Metallic Substrates: Systematic Investigation of Surface Plasmon Resonance and Surface-Enhanced Raman Scattering. *J. Phys. Chem. B.* **2006,** *110*, 17444-17451.

10. Sylvestre, J.-P.; Poulin, S.; Kabshin, A. V.; Sacher, E. M., M.; Luong, J. H. T., Surface Chemistry of Gold Nanoparticles Produced by Laser Ablation in Aqueous Media. *J. Phys. Chem. B.* **2004,** *108*, 16864-16869.

11. McBride, J. R.; Pennycook, T. J.; Pennycook, S. J.; Rosenthal, S. J., The Possibility and Implications of Dynamic Nanoparticle Surfaces. *ACS Nano* **2013**, Article ASAP.

12. Frens, G., Controlled Nucleation for the Regulation of the Particle Size in Monodisperse Gold Suspensions. *Nature: Phys. Sci.* **1973,** *241*, 20-22.

13. Coskun, S.; Aksoy, B.; Unalan, H. E., Polyol Synthesis of Silver Nanowires: An Extensive Parametric Study. *Cryst. Growth Des.* **2011,** *11*, 4963-4969.

14. Song, J.; Wang, X.; Riedo, E.; Wang, Z. L., *Nano Lett.* **2005,** *5*, 1954.

15. Yang, Q. Z.; Huang, Z.; Kucharski, T. J.; Khvostichenko, D.; Chen, J.; Boulatov, R., *Nat. Nano.* **2009,** *4*, 302.

16. Demczyk, B. G.; Wang, Y. M.; Cumings, J.; Hetman, M.; Han, W.; Zettl, A.; Ritchie, R. O., *Mat. Sci. Eng. A - Struct.* **2002,** *334*, 173.

17. Simeone, F. C.; Albonetti, C.; Cavallini, M., *J. Phys. Chem. C* **2009,** *113*, 18987.

18. Jang, D. C.; Greer, J. R., *Nat. Mater.* **2010,** *9*, 215.

19. William D. Callister, J.; Rethwisch, D. G., *Materials Science and Engineering An Introduction*. 8 ed.; John Wiley and Sons, Inc.: Hoboken, NJ, 2010; 885.

20. Hostetler, M. J.; Templeton, A. C.; Murray, R. W., *Langmuir* **1999,** *15*, 3782.

21. Wong, E. W.; Sheehan, P. E.; Lieber, C. M., *Science* **1997,** *277*, 1971.

22. Yu, M. F.; Lourie, O.; Dyer, M. J.; Moloni, K.; Kelly, T. F.; Ruoff, R. S., *Science* **2000,** *287*, 637.

23. Salvetat, J. P.; Kulik, A. J.; Bonard, J. M.; Andrew, G.; Briggs, D.; Sto¨ckli, T. M. t. n., K.; Bonnamy, S. B. g., F.; Burnham, N. A.; Forro´, L., *Adv. Mater* **1999,** *11*, 161.

24. Salvetat, J. P.; Andrew, G.; Briggs, D.; Bonard, J. M.; Bacsa, R. R.; Kulik, A. J.; Sto¨ckli, T.; Burnham, N. A.; Forro´, L. s., *Phys. Rev. Lett* **1999,** *82*, 944.

25. Chao Wang; Yujie Wei, H. J.; Sun, S., Bending Nanowire Growth in Solution by Mechanical Disturbance. *Nano Lett.* **2010,** *10*, 2121-2125.

26. Xun Hong; Dingsheng Wang; Li, Y., Kinked gold nanowires and their SPR/SERS properties. *Chem. Comm.* **2011,** *47*, 9909–9911.

27. Van Helden, A. K.; Jansen, J. W.; Vrij, A., Preparation and characterization of spherical monodisperse silica dispersions in nonaqueous solvents. *J. Colloid Interface Sci.* **1981,** *81*, 354.

28. Badley, R. D.; Ford, W. T.; McEnroe, F. J.; Assink, R. A., Surface modification of colloidal silica. *Langmuir* **1990,** *6*, 792.

29. Bogush, G. H.; Zukoski IV, C. F., *Ultrastructure Processing of Advanced Ceramics*. Wiley: New York, 1988.

30. Stober, W.; Fink, A., Controlled Growth of Monodisperse Silica Spheres in the Micron Size Range. *J. Colloid Interface Sci.* **1968,** *26*, 62.69.

31. G, C.; G, D., *Polymer* **1981,** *22* 1181-1189.

32. Schild, H. G., Poly(N-isopropylacrylamide): experiment, theory and application. *Progress in Polymer Science* **1992,** *17* (2), 163-249.

33. Heskins, M.; Guillet, J. E., *Macromol. Sci. Chem. A* **1968,** *2*, 1441.

34. Wu, C.; X., W., Globule-to-Coil Transition of a Single Homopolymer Chain in Solution. *Phys. Rev. Lett.* **1998,** *80* (18), 4092-4094.

35. Chung, J. E.; Yokoyama, M.; Yamato, M.; Aoyagi, T.; Sakurai, Y.; Okano, T., Thermo-responsive drug delivery from polymeric micelles constructed using block copolymers of poly(N-isopropylacrylamide) and poly(butylmethacrylate). *Journal of Controlled Release* **1999,** *62* (115-127).

36. François Ganachaud; Michael J. Monteiro; Robert G. Gilbert; Marie-Anne Dourges; San H. Thang; Rizzardo, E., Molecular Weight Characterization of Poly(N-isopropylacrylamide) Prepared by Living Free-Radical Polymerization. *Macromolecules* **2000,** *33* (18), 6738-6745.

37. Teresa López-León; Juan L. Ortega-Vinuesa; Delfi Bastos-González; Elaïssari, A., Cationic and Anionic Poly(N-isopropylacrylamide) Based Submicron Gel Particles: Electrokinetic Properties and Colloidal Stability. *J. Phys. Chem. B* **2006,** *110* (10), 4629-4636.

38. Halasa, A. F., *Rubber Chem. Technol.* **1981,** *54*, 627.

39. Wang, J.; Matyjaszewski, K., Controlled/"living" radical polymerization. Atom transfer radical polymerization in the presence of transition-metal complexes. *J. Am. Chem. Soc.* **1995,** *117*, 5614-5615.

40. Cowie, J. M. G.; Arrighi, V., I. In *In Polymers: Chemistry and Physics of Modern Materials*, 3rd edition ed.; CRC Press Taylor and Francis Group: Boca Raton, Fl, 2008; pp 82-84.

41. Kato, M.; Kamigaito, M.; Sawamoto, M.; Higashimura, T., Polymerization of Methyl Methacrylate with the Carbon Tetrachloride/Dichlorotris-(triphenylphosphine)ruthenium(II)/Methylaluminum Bis(2,6-di-tert-butylphenoxide) Initiating System: Possibility of Living Radical Polymerization. *Macromolecules* **1995,** *28*, 1721-1723.

42. Patten, T. E.; Matyjaszewski, K., Atom Transfer Radical Polymerization and the Synthesis of Polymeric Materials. *Adv. Mater.* **1998,** *10*, 901.

43. Matyjaszewski, K.; Xia, J., Atom Transfer Radical Polymerization. *Chem. Rev.* **2001,** *101* (9), 2921-2990.

44. Odian, G., In *In Radical Chain Polymerization; Principles of Polymerization*, Wiley-Interscience: Staten Island, New York, **2004**; 316–321.

45. Robert H. Lambeth; Subramanian Ramakrishnan; Ryan Mueller; John P. Poziemski; George S. Miguel; Larry J. Markoski; Charles F. Zukoski; Moore, J. S., Synthesis and Aggregation Behavior of Thermally Responsive Star Polymers. *Langmuir* **2006,** *22* (14), 6352-6360.

46. Kelly, K. L.; Coronado, E.; Zhao, L. L.; Schatz, G. C., *J. Phys. Chem. B.* **2003,** *107*, 668.

47. Jain, P. K.; Huang, X.; El-Sayed, I. H.; El-Sayad, M. A., *Plasmonics* **2007,** *2*, 107.

48. Alivisatos, A. P., *J. Phys. Chem.* **1996,** *100*, 13226.

49. Niemeyer, C. M., *Angew. Chem. Int. Ed.* **2001**. *40*, 4128.

50. Murphy, C. J.; Gole, A. M.; Stone, J. W.; Sisco, P. N.; Alkilany, A. M.; Goldsmith, E. C.; Baxter, S. C., *Acc. Chem. Res.* **2008,** *41*, 1721.

51. Wu, T.; Zhang, Y.; Wang, X.; Liu, S., Fabrication of Hybrid Silica Nanoparticles Densely Grafted with Thermoresponsive Poly(N-isopropylacrylamide) Brushes of Controlled Thickness via Surface-Initiated Atom Transfer Radical Polymerization. *Chem. Mater.* **2007,** *20*, 101-109.

52. Wu, T.; Zhang, Q.; Hu, J.; Zhang, G.; Liu, S., Composite silica nanospheres covalently anchored with gold nanoparticles at the outer periphery of thermoresponsive polymer brushes. *J. Mater. Chem.* **2012,** *22*, 5155-5163.

53. Lu, Z.; Sun, L.; Nguyen, K.; Gao, C.; Yin, Y., Formation Mechanism and Size COntrol in One-Pot Synthesis of Mercapto-Silica Colloidal Spheres. *Langmuir* **2011,** *27*, 3372-3380.

54. Atwood, J. L., Inclusion Compounds. In *Ullmann's Encyclopedia of Industrial Chemistry*, Wiley: VCH, Weinheim, 2012.

55. Saunders, B., Responsive Microgel Dispersions. In *Encyclopedia of Surface and Colloid Science*, Somasundara, P., Ed. Taylor and Francis: Vol. 5. 2006.

56. Howard G. Schild; M. Muthukumar; Tirrell, D. A., Cononsolvency in mixed aqueous solutions of poly(N-isopropylacrylamide). *Macromolecules* **1991,** *24* (4), 948-952.

57. Christian H. Hofmann; Felix A. Plamper ; Christine Scherzinger ; Sami Hietala; Richtering, W., Cononsolvency Revisited: Solvent Entrapment by N-Isopropylacrylamide and N,N-Diethylacrylamide Microgels in Different Water/Methanol Mixtures. *Macromolecules* **2013,** *46* (2), 523-532.

58. Siegwart, D. J.; Oh, J. K.; Gao, H.; Bencherif, S. A.; Perineau, F.; Bohaty, A. K.; Hollinger, J. O.; Matyjaszewski, K., Biotin-, Pyrene-, and GRGDS-Functionalized Polymers and Nanogels via ATRP and End Group Modification. *Macromol. Chem. Phys.* **2008,** *209*, 2179-2193.

59. Anderluh, G.; Lakey, J. H., *Membrane Binding and Pore Formation*. Springer: New York, Vol. 677; **2010**.

60. Porter, M. D.; Bright, T. B.; Allara, D. L.; Chidsey, C. E. D., Spontaneously Organized Molecular Assemblies. *J. Am. Chem. Soc.* **1987,** *109*, 3559-3568.

61. Fultz, B.; Howe, J.; Howe, J. M., *Transmission Electron Microscopy and Diffractometry of Materials*. 3rd Edition ed.; Springer: New York, 2007.

62. Wang, Y.; Zhong, M.; Zhang, Y.; Magenau, A. J. D.; Matyjaszewski, K., Halogen Conservstion in Atom Transfer Radical Polymerization. *Macromolecules* **2012,** *45*, 8929-8932.

63. Hong, S. C.; Lutz, J.-F.; Inoue, Y.; Strissel, C.; Nuyken, O.; Matyjaszewski, K., Use of an Immobilized/Soluble Hybrid ATRP Catalyst System for the Preparation of Block Copolymers, Random Copolymers, and Polymers with High Degree of Chain End Functionality. *Macromolecules* **2003,** *36* 1075-1082.

64. Jakubowski, W.; Kirci-Denizli, B.; Gil, R. R.; Matyjaszewski, K., Polystyrene with Improved Chain-End Functionality and Higher Molecular Weight by ARGET ATRP. *Macromol.Chem. Phys.* **2008,** *209*, 32-39.

65. Lutz, J.-F.; Matyjaszewski, K., Kinetic Modeling of the Chain-End Functionality in Atom Transfer Radical Polymerization. *Macromol. Chem. Phys.* **2002,** *203*, 1385-1395.

66. Smela, E., *Adv. Mater* **2003,** *15*, 481.